Copernicus Climate Change

Integration of Climate Data in the SAVi Nature-Based Infrastructure Model

C3S_428h_IISD-EU: Sustainable Asset Valuation (SAVi): Demonstrating the Business Case for Climate-Resilient and Sustainable Infrastructure

Issued by: IISD-EU / Oshani Perera

Date: September 2020

Ref:

C3S_428h_IISD-EU_D428h.1.1 _202006_Integration of climate data in the SAVi model_v2

Official reference number service contract:

2019/C3S_428h_IISD-EU/SC1

IMPLEMENTED BY ECMWF

Contributors

International Institute for Sustainable Development
Bechauf, Ronja
Casier, Liesbeth
Lago, Sergio
Perera, Oshani
Perrette, Mahé
Uzsoki, David
Wuennenberg, Laurin

KnowlEdge Srl
Bassi, Andrea M.
Pallaske, Georg

Table of Contents

1 About this paper 5

2 Nature-based Infrastructure 8

2.1 Literature review 8
2.1.1 Definitions 8
2.1.1.1 Natural Infrastructure 8
2.1.1.2 Green-Grey infrastructure 8
2.1.2 Precipitation: rainfall harvesting, runoff 8
2.1.3 Vegetation: rainfall absorption, temperature, soil erosion and climate mitigation 11
2.1.4 Air temperature and solar radiation 13
2.2 Integration of literature review with the CDS datasets 18
2.3 Integration of climate indicators into the SAVi natural infrastructure model 19
2.4 Behavioral impacts resulting from the integration of climate variables 20
2.5 Simulation results 21
2.5.1 Effect of temperature on P removal efficiency in wetlands 21
2.5.2 Effect of temperature on labor productivity and impacts of vegetation cover 23
2.5.3 Impacts of vegetation cover on surrounding air temperature 24

3 Bibliography 26

Annex I: Code for establishing the CDS Toolbox-SAVi link 37

How does this code relate to the CDS API ? 37
Code available for download 37
Installation steps 37
CDS API 38
Indicator definition 39
Netcdf to csv conversion 41

1 About this Report

This report outlines the integration of authoritative Copernicus Climate Data from the Climate Data Store (CDS) into a Sustainable Asset Valuation (SAVi) of nature-based infrastructure. It describes how several climate indicators obtained from the Copernicus CDS were integrated into the SAVi Nature-Based Infrastructure model and how the analysis performed by SAVi has improved as a result. In light of this integration, IISD is able to generate sophisticated SAVi-derived analyses on the costs of climate-related risks and climate-related externalities.

The integration of Copernicus Climate Data into other SAVi models for energy, irrigation, wastewater treatment infrastructure, buildings, and roads can be found here.

This document presents

- A summary of the literature review on the climate impact on nature-based infrastructure, including equations that link climate variables to the performance of nature-based infrastructure.
- How the above information was used to select relevant indicators from the Copernicus database.
- How outputs of the CDS datasets are integrated into the SAVi System Dynamics (SD) Nature-Based Infrastructure model.
- How simulation results can be affected by the use of this new and improved set of indicators.

This report is organized as follows.

Literature Review

The literature review contains the following subsections for each of the climate variables discussed for nature-based infrastructure:

- Subsection 1: An overview of climate impacts on the asset (e.g., temperature affects natural infrastructure).
- Subsection 2: A presentation of papers/reports that provide case studies that summarize the range of impacts estimated or observed (e.g., across countries).
- Subsection 3: A description of the methodology found in the literature for the calculation of climate impacts on the infrastructure asset.
- Subsection 4: A selection of CDS datasets required by the equations.

Integration of the Literature Review With the CDS Dataset

This section summarizes information on what datasets are being used from the Copernicus database and what additional processing was applied before integration into the SAVi Nature-

Based Infrastructure model. We first review equations to determine their usefulness for SAVi models. We then assess what data requirements for each of the equations are available in the Copernicus database and create indicators for climate variables that are relevant for the equations selected. Finally, in certain cases, we create indicators in the CDS Toolbox for first-order impacts on infrastructure. Second- and third-order impacts will be estimated with SAVi, making use of additional equations included in the SD model.

Integration of Climate Indicators Into the SAVi Nature-Based Infrastructure Model

This section explains how the CDS indicators are used in the SAVi SD model for nature-based infrastructure. it includes an identification of specific performance indicators for each asset impacted by climate indicators (e.g., efficiency and cost).

Behavioural Impacts Resulting From the Integration of Climate Variables

This sections discusses how the climate variables affect asset performance in the SD model, providing early insights as to how the results of the SAVi analysis may change when equipping the model with more and better refined climate indicators (e.g. cost of infrastructure being higher due to increased maintenance, the economic viability of the infrastructure asset, expressed as the Internal Rate of Return (IRR), will be lower than expected).

Simulation Results

The final section of this paper presents equations used and quantitative results emerging from the inclusion of climate indicators in the SAVi Nature-Based Infrastructure model under various climate scenarios. This is the end product of the enhanced SAVi model, which is used to inform policy and investment decisions for infrastructure. Table 1 provides an overview of climate drivers, impacts, and relevant SAVi output indicators.

The CDS datasets are accessed via the CDS application programming interface (API), and additional processing and packaging for use in SAVi is done offline. Technical information about the offline code is found in Annex I. We also selected a subset of the most-used indicators and created an app in the CDS Toolbox with interactive visualization for demonstration purposes.

Table 1. Overview of variables and impacts implemented in the SAVi Nature-based Infrastructure model

SAVi module	Implemented impact	Main climate drivers	Affected output indicators
Nature-based infrastructure	Labour productivity impact indicator	• Temperature	• Months with potential labour productivity impacts
	Air temperature considering vegetation cover	• Temperature	• Effect of 25%, 50%, and 75% vegetation cover

SAVi module	Implemented impact	Main climate drivers	Affected output indicators
			• Labour productivity impact indicator

2 Nature-based Infrastructure

2.1 Literature review

2.1.1 Definitions

2.1.1.1 Natural Infrastructure

Natural infrastructure is defined as ecosystems that provide infrastructure through services that are inherent to such ecosystems, while also perpetuating active conservation efforts and the enhancement of the environments they are embedded in. (Bassi, Pallaske, Wuennenberg, Graces, & Silber, 2019)

2.1.1.2 Green-Grey infrastructure

Green-grey infrastructure is an urbanized natural infrastructure; it tends to hybridize natural and grey infrastructure into easily implementable structures to urban environments (e.g., permeable pavements, green spaces). (Bassi, Pallaske, Wuennenberg, Graces, & Silber, 2019)

2.1.2 Precipitation: rainfall harvesting, runoff

- **Climate impact**

Precipitation is one of the main climate variables that impacts natural and green-grey infrastructure. It affects rainwater harvesting, water management and water absorption through vegetation or soils. Natural and green-gray infrastructures can reduce extreme events impacts on buildings (reducing flood impact), curb demand for water (rainwater harvesting) and improve the performance of wastewater plants. They also are good to treat and absorb high precipitation as well as wastewater through constructed or natural wetlands and mangroves, among others.

- **Summary of results**

Green roofs have a capacity of retaining 75% of a 24.5mm storm and 85% from a 50.8mm storm (depending on location, results are for Chicago and Milwaukee respectively). In comparison with asphalt, we also found that for recorded precipitation of 323mm on average for green roofs and 587mm for asphalt roofs, they respectively retained 52.6% and 14.1%. For pavements, we found that the efficiency of retaining a 1-hour storm is 3mm.
For a Combined Sewer Overflow, there would be a reduction in discharge of 2.8391 liters (0.75 US gallon) per increase of 3.7854 liters (1 US gallon) of stormwater when we install a green infrastructure near the water inflow.
In a study in Spain, comparing constructed wetlands in Barcelona and Leon regarding their respective seasonal efficiency removal, it was found that for [TSS; COD; ammonium], their efficiency in summer is [97.4%-97.8%; 97.1%-96.2%; 99.9%-88.9%] and winter [83.5%-74.4%; 73.2%-60.6%; 19%-NA] respectively for Barcelona and Leon. Influent average TSS mass loading rate was 2.84 g m^{-2} d^{-1} and for average influent BOD, it was of 4.72 g m^{-2} d^{-1}.

- **Results**

In Chicago, green roofs helped retain over 75 percent of the volume from a one-inch storm, preventing the water from reaching the combined sewer system. In Milwaukee, green roofs will be able to retain 85 percent of a two-inch downpour. The remaining 15 percent of the water is directed to rain gardens and a retention basin for on-site irrigation. (Dunn, 2007)

In the US, a report published under the NRDC by Kloss and Calarusse (2011),established that permeable pavement in a typical alley can infiltrate 3 inches of rainwater from a 1-hour storm with an infrastructure life expectancy of 30 to 35 years. It is typically designed with the capacity to manage a 10-year rain event within a 24-hour period.

Under the EPA, Berghage et al. (2009) reported in an analysis across the US that for 683 mm of recorded precipitation, there was a corresponding mean value of 323 mm with a standard deviation of 71 mm of green roof runoff compared to a mean of 587 mm with a calculated standard deviation of 43 mm for the flat asphalt roofs. The green roofs retained 52.6% while flat asphalt roofs retained 14.1% of the precipitation.

In Lancaster, Pennsylvania, a project managed by the Green Infrastructure Technical Assistance Program and the EPA, estimated that for every 1 gallon of stormwater captured by green infrastructure, (Combined Sewer Overflow) CSO discharges will be reduced by 0.75 gallons. Based on these assumptions, the green infrastructure installed within the CSS area will capture an average of 706 million gallons of stormwater runoff annually, and reduce CSO discharges by an average of 529 million gallons/year. (EPA, 2014)

In Spain, Garfi et al. (2012) estimated the removal efficiency of two experimental constructed wetlands in Leon and Barcelona. The two constructed wetland systems had the same experimental set-up. Each wetland had a surface area of 2.95 m^2, a water depth of 25 cm and a granular medium of D60=7.3 mm, and was planted with Phragmites australis. Both systems were designed in order to operate with a maximum organic loading rate of 6 gDBO m^{-2} d^{-1}. Experimental systems operated with a hydraulic loading rate of 28.5 and 98 mm d^{-1} in Barcelona and León, respectively. Total suspended solids, biochemical oxygen demand and ammonium mass removal efficiencies followed seasonal trends, with higher values in the summer (97.4% vs. 97.8%; 97.1% vs. 96.2%; 99.9% vs. 88.9%, in Barcelona and León systems, respectively) than in the winter (83.5% vs. 74.4%; 73.2% vs. 60.6%; 19% vs. no net removal for ammonium in Barcelona and León systems, respectively).

Influent average TSS mass loading rate was 2.84 g m^{-2} d^{-1} (7.58 g m^{-2} d^{-1}, ranging from 0.41 to 7.95 g m^{-2} d^{-1} in Leon). Average influent BOD was 4.72 g m^{-2} d^{-1} (6.11 g m^{-2} d^{-1} in Leon), ranging from 3.5 to 5.1 g m^{-2} d^{-1} in winter and summer respectively, which fits quite well in the range of 4–6gm^{-2} d^{-1}.

- **Methodology**

Many papers are based on the same methodology, the SWMM (StormWaterManagement Method) (Nazahiyah, Yusop, & Abustan, 2007). See the article of Zoppou (2001) for all the listed urban stormwater models. One of the first examples is the article of Tsihrintzis and Hamid (1998).

This approach allows to know how much pollutants were absorbed through runoff and probably not treated. Pollutant loadings were calculated as the product of event mean concentration (EMC):

$$\mathrm{EMC} = \frac{M}{V} = \frac{\sum Q_i C_i \Delta t}{\sum Q_i \Delta t}$$

where M is total mass of pollutant over the entire event duration (g), V is total volume of flow over the entire event duration (m3), t is time (min), Qi(t) is the time-variable flow (m3 /min), Ci is the time-variable concentration (mg/l) and Dt is the discrete time interval (min) measured during the runoff event.

<u>Considerations for integration in the CDS toolbox</u>

ERA5-Land monthly averaged data from 1981 to present
CMIP5 monthly data on single levels

<u>Method 2</u> (Gajbhiye, Mishra, & Pandey, 2013) (Cronshey, et al., 1986)

This method is based on the Soil Conservation Service curve number (CN) Method, a well-established technique for estimating event runoff depths from various urban and agricultural land uses. The CN method uses an infiltration loss model to estimate direct runoff from storm rainfall based on soil type, land use/land cover, surface conditions, and antecedent moisture conditions:

$$VR = \frac{(P - Ia)^2}{P - Ia + S} \cdot A_d \cdot C$$

and

P = total event precipitation depth, [in]
$S = \frac{1000}{\mathrm{CN}} - 10$
CN = curve number, set at 98 for impervious urban surfaces
Ia = initial abstraction, $0.2\,S$
A_d = Drainage area (m^2)
C = conversion factor from inches to m.

Initial abstraction (Ia) is all losses before runoff begins. It includes water retained in surface depressions, water intercepted by vegetation, evaporation, and infiltration. Ia is highly variable but generally is correlated with soil and cover parameters. Through studies of many small agricultural watersheds, Ia was found to be approximated by the following empirical equation:
Ia = 0,2S

The major factors that determine CN are the hydrologic soil group (HSG), cover type, treatment, hydrologic condition, and antecedent runoff condition (ARC)

Considerations for integration in the CDS toolbox

ERA5-Land monthly averaged data from 1981 to present
CMIP5 monthly data on single levels

2.1.3 Vegetation: rainfall absorption, temperature, soil erosion and climate mitigation

- **Climate impact**

Vegetation has an impact on natural and green-grey infrastructure depending on the type of vegetation, country, latitude, and canopy coverage. Vegetation helps mitigating climate risks on infrastructure and provides an efficient way of increasing air quality, reducing flood risks, absorbing high precipitation levels, and reducing the demand for cooling.

- **Summary of results**

Our references mainly come from studies in the US, China and England.
Trees are important in mitigating flood and wastewater treatment costs by their rainfall absorption capacity. We found that trees can absorb as much as 6.6 m^3/tree and reduce costs by 3.6$/tree (Santa Monica). Trees also act as air cleaner by reducing air pollutants. In some studies they found that for PM2.5 removal, trees could reduce it by ~64.5 tons (Atlanta) and for nitrogen, sulfur dioxide and total suspended particulates altogether, around 312.03 tons (Guangzhou) depending on location. For example, a 10 x 10 km grid in London with 25% tree cover could remove 90.4 tons of PM10 per year
For vegetated areas, we learned that they are 3% cooler than non-vegetated areas (Kumamoto, Japan). For example, a 30% vegetated area can be cooler by 6˚C, retain warmth at night by 2˚C and reduce wind speed by 2-6.7 m/s (Davies, California). Vegetation also prevents soil erosion. We found that for a 1% annual increase in vegetation cover, soil erosion could be reduced by 456 t/km^2/a^{-1} (China).
We also found that on average, vegetation can absorb carbon particles by 18 to 31.6 t ˚C/ha depending on location for urban areas and as much as 1.66-7.6 t ˚C/ha for domestic gardens (Leicester). For removal efficiency, depending on location the removal of PM10/year ranges from 852 to 2121 tons (Seattle and Hangzhou).

- **Results**

In Santa Monica, California, Xiao and McPherson (2002) assessed the rainfall absorption capacity of urban trees to mitigate wastewater treatment costs and flood costs. Results show that the annual rainfall interception by the 29,299 street and park trees was 193,168 m^3 (6.6 m^3/tree), or 1.6% of total precipitation. Longtime average annual precipitation is 569.5 mm and the dominant

land use over the 21.8 km^2 study area is residential (66.0%). Commercial, industrial, and park land uses account for 15.9%, 7.0%, and 2.6%, respectively. The remaining 8.5% of land has other uses. Inventory data was limited to 29,229 public trees, of which 87% were street trees and 13% were park trees. The majority of trees were broadleaf evergreens (59.9%), 11.1% were conifers, and 22.6% were palms
The annual value of avoided stormwater treatment and flood control costs associated with reduced runoff was $110,890 ($3.60/tree). Interception rate varied with tree species and sizes.

In Kumamoto, Japan, Saito et al. (1990) estimated the impact of vegetation coverage on air temperature. Temperature difference is on average 3% lower compared to non-vegetated areas. Three areas were analyzed. The Kengun Shinto Shrine area has a scale of about 150m × 150m and it is covered with coniferous trees and bamboos. The Izumigaoka Park has a scale of about 60m × 40 m and it is covered with broad-leaved trees. The total area of tree crowns is ~25 900 m^2 in Kengun Shinto Shrine and ~2300 m^2 in Izumigaoka Park.

In Davis, California, Taha et al. (1991) estimated that a vegetative cover of 30% could produce a noontime oasis of up to 6°C in favorable conditions, and a nighttime heat island of 2°C. Wind speed was reduced by ~ 2 m/s in mild conditions and by as much as 6.7 m/s. The measurements were taken from 12 to 25 October 1986. These meteorological variables were measured 1.5 m above ground along a transect of 7 weather stations set up across the canopy and the upwind/downwind open fields. These variables were averaged every 15 minutes for a period of two weeks so we could analyze their diurnal cycles as well as their spatial variability. In the canopy, the cumulative leaf-area index (LAI), integrated over the foliage depth, was about 3. This LAI was uniform across the entire canopy except near the middle of the tree stand where a slight discontinuity in cover brought the LAI down to about 2. The tall trees at the south end of the stand, on the other hand, had a cumulative LAI between 4.5 and 5.

In China, Zhou et al. (2006) assessed the evolution of vegetation and soil erosion at the watershed of Zhifanggou from 1987 to 1996. Vegetation coverage increased linearly with a speed of 1.84% per year and soil erosion decreased by 757 t km^{-2} per year. The amount of soil erosion was closely negative correlated with the degree of vegetation coverage ($r = -0.99^{***}$). Regression of soil erosion with vegetation coverage indicated that a 1% increase in vegetation coverage in a year could decrease soil erosion by 456 t km^{-2} a^{-1}.

Demuzere et al. (2014) also reported existing evidence on the role of green infrastructures in mitigating climate change.
For Co2 reduction Davies et al (2011) reported the total average carbon stored within the above-ground vegetation across the city to be 31.6 t C/ha of urban area and 7.6 t C/ha alone for domestic gardens.
This is similar to the results of Zhao et al. (2010)in the Hangzhou downtown area, where they reported 30.25 t C/ha and 1.66 t C/ha/year as the average carbon storage and sequestration rate, and a little higher than along three sample transects radiating from the Seattle (the USA) central urban core (18 ± 13.7 t C/ha) (Hutyra, Yoon, & Alberti, 2011).

Concerning air quality, the evidence based on modeling studies is much broader compared to the results from empirical studies. In London, green areas are estimated to remove 852-2121 tons of PM10 annually, which equates to 0.7-1.4% PM10 reduction (Tiwary, et al., 2009).
Tallis et al. (2011) have found that a 10 x 10 km grid in London with 25% tree cover could remove 90.4 tons of PM10 per year.
A recent analysis in 10 US cities showed that the mass of fine particles (PM2.5) removed by trees annually could be up to 64.5 tons in Atlanta (Nowak, Greenfield, Hoehn, & Lapoint, 2013).
In Guangzhou, China, the annual removal of nitrogen, and sulfur dioxide and total suspended particulates could be 312.03 tons. (Jim & Chen, 2008)

- **Methodology**

Considerations for integration in the CDS toolbox

ERA5-Land monthly averaged data from 1981 to present
ERA5 monthly averaged data on single levels from 1979 to present
Land cover classification gridded maps from 1992 to present derived from satellite observations
ERA5-Land monthly averaged data from 1981 to present
Leaf area index and fraction absorbed of photosynthetically active radiation 10-daily gridded data from 1981 to present

2.1.4 Air temperature and solar radiation

- **Climate impact**

Green roofs and green gardens, among other options, can provide a good alternative for cities to face higher temperatures and decrease the demand for cooling. They can also act as greenhouse gas emissions regulators and contribute to the improvement of air quality.
As for air temperatures, green-gray infrastructures allow to reduce solar radiation impact on buildings. They help in reducing demand for cooling systems and can even transform solar radiation energy into electricity through solar panels.
Constructed and natural wetlands are also sensitive to changes in temperatures regarding their nutrient absorption efficiency and their capacity in treating wastewater.

- **Summary of results**

An increase in Albedo of 0.13 would lead to a decrease of temperature by 2-4 ˚C and hence, reduce air conditioning need by 10% and reduce smog by 20% during summer.
Trees help mitigating high temperatures. By doing a simple average from all our references, areas with trees are cooler by 2.15˚C (0.7 – 3.6 ˚C range of our studies) depending on location, method. Green areas also help reducing ambient air temperature by an average of 1.635˚C (0.47-2.8˚C range) to a most of 3.3-5.6˚C for +25% of trees.

Green roofs have the same function as trees. We found that it could reduce ambient air temperature by 0.3-3˚C and facades temperature by 1-15˚C. Its surface temperature can be lower by 21˚C and it can reduce air temperature by 15˚C for another more extreme study.
Regarding green infrastructure and constructed wetlands, their efficiency of water treatment also changes with temperature variation. COD removal is relatively high at 16˚C (92%) and at 24˚C in (88%), but ranged between 58% and 69% during all other batches at 4, 8, and 16˚C. Removal rate without plants was significantly less at 4˚C than 24˚C. At 4 and 8˚C, when differences were statistically significant, planted microcosms removed 25–30% more COD on average than unplanted controls; at 16˚C, significant differences between planted and unplanted microcosms were <20%. For absorption in another study, the average Nitrogen uptake rate was calculated in the order of *C. indica L. > A. donax > A. calamus L.*, for 22.88 mgN/m^3 /d, 18.21 mgN/m^3 /d and 16.68 mgN/m^3 /d, respectively. NO3-N removal rates of 95.2%, 97.2%, 96.8% and 96.2% occurred in summer (Aug. and Sep.), while 83.3%, 84.4%, 77.56% and 73.45% in autumn (Oct. to Dec.).
For wetland without specific plant, removal efficiency was for SS (71.8 ± 8.4%), BOD5 (70.4 ± 9.6%), COD (62.2 ± 10.1%), total coliform (99.7%), fecal coliform (99.6%), ammonia nitrogen was relatively low (40.6 ± 15.3%).
For inflow and removal efficiency per year the wetland received 24 g P m^{-2} $year^{-1}$ and 130 g NO3–N m^{-2} $year^{-1}$ and it retained 3.1 g m^{-2} $year^{-1}$ of P and 18 g m^{-2} $year^{-1}$ of NO3–N. Annual TP reduction was 13% and NO3–N reduction 14%. The monthly relative NO_3–N reduction was 25–82% in growing season (June–September), 7–10% in January–March and 4–6% in November–December. The highest absolute monthly reduction of NO_3–N occurred in December.
For specific regional climate, look at figure 39 below.

- **Results**

Two studies led by Taha in (1996) and in (1997) in the Los Angeles basin performed simulations of the effects of large scale albedo increases and found that an average decrease of 2°C and up to 4°C may be possible by increasing the albedo by 0.13 in urbanized areas of the basin. Temperature decreases of this magnitude could reduce the electricity load from air conditioning by 10% and smog (ozone concentrations) by up to 20% during a hot summer day.

A paper assessing the vegetation role in mitigating urban heat island in Athens, elaborated by Zoulia et al. (2009) shows that air temperature in the shade of trees was reported to be lower by 0.7–1.3°C (Souch & Souch, 1993)*)*, 1.7–3.3°C (Taha, Akbari, & Rosenfeld, 1988),up to 3.6°C (Parker, 1989)than areas with no trees. The cooling effect of parks was also investigated by several other researchers: the average air temperature in green areas was recorded to be lower by 0.47°C (Dhakal & Hanaki, 2002), 0.6°C (Watkins, Littlefair, Kolokotroni, & Palmer, 2002), 1.5–2.8°C (Nichol, 1996) than surrounding areas.
In another study, this temperature difference reached up to 3.3– 5.6°C during summer with a 25% increase in the number of trees. (Akbari, Davis, Dorsano, Huang, & Winnett, 1992)

Koc et al. (2018) did a literature review on the effects of green infrastructures for cooling urban areas:
It is said that green roofs, when applied at the city level, may decrease average ambient temperatures between 0.3 and 3 K (Santamouris, 2014) and also that the application of green

walls/facades showed a reduction of surface temperatures of building facades between 1 and 15 °C for studies in warm temperate climates (Pérez, Coma, Martorell, & Cabeza, 2014). This is just two examples among many others.

In a report published by the EPA in 2003, in the US, it is estimated that urban air temperatures can be up to 5.6 C warmer than the surrounding countryside and for every 0.6˚C increase in air temperature, peak utility load may increase by 2%. (U.S. Environmental Protection Agency, 2003)

In Chicago, since its completion in 2001, green roofs have saved the city USD 5,000 a year in energy costs (City of Chicago Department of Environment, 2006). Monitoring of local temperatures found that the "cooling effects during the garden's first summer showed a roof surface temperature reduction of 21°C and an air temperature reduction of 15°C (American Society of Landscape Architects, 2003) .

Taylor et al. (2011) conducted a study on the efficiency of 19 different plants in absorbing and removing COD and SO_4 from wastewater under different air temperatures. They compared treatment and control (unplanted) by varying temperatures after 20 days during 1 year.
In unplanted microcosms COD removal was relatively high at 16◦C in 2006 (92%) and at 24 ◦C in 2007 (88%), but ranged between 58% and 69% during all other batches at 4, 8, and 16 ◦C. Removal in controls was significantly less at 4◦C than 24 ◦C. In contrast to the controls, planted microcosms showed no significant differences between the coldest and warmest temperatures with 15 species. Microcosms planted with *L.cinereus* and *P. virgatum* had significantly lower COD removal at 4 than 24 ◦C, while *C. utriculata* and *P. arundinacea* had significantly higher removal at 4 ◦C.
At 4 and 8 ◦C, when differences were statistically significant, planted microcosms removed 25–30% more COD on average than unplanted controls; at 16 ◦C, significant differences between planted and unplanted microcosms were <20%. We can clearly see it in a table available in the article:

Figure 1 – COD removal regarding influent wastwater

COD removal in wetland microcosms as percent reduction relative to influent wastewater (±standard error).

	16 °C 2006[b]	8 °C 2006	4 °C 2007	8 °C 2007	16 °C 2007	24 °C 2007	16 °C 2007	8 °C 2007	4 °C 2008	Study-long average[c]
D. cespitosa	95 ± 2	99 ± 1 ↑	99 ± 1 ↑	98 ± 1 ↑	100 ± 0 ↑	96 ± 2	95 ± 1 ↑	95 ± 1 ↑	98 ± 1 ↑	97 ± 2
C. bebbii	90 ± 2	98 ± 1 ↑	98 ± 1 ↑	98 ± 0 ↑	99 ± 0 ↑	100 ± 0 ↑	91 ± 2 ↑	99 ± 0 ↑	98 ± 1 ↑	97 ± 1
C. nebrascensis	91 ± 2	100 ± 0 ↑	96 ± 2 ↑	98 ± 1 ↑	96 ± 3 ↑	93 ± 3	95 ± 0 ↑	99 ± 0 ↑	97 ± 1 ↑	96 ± 1
C. praegracilis	96 ± 1	95 ± 2 ↑	NA	97 ± 1 ↑	95 ± 2 ↑	97 ± 3	94 ± 1 ↑	98 ± 2 ↑	97 ± 1 ↑	96 ± 1
S. acutus	87 ± 3	92 ± 5 ↑	92 ± 2 ↑	94 ± 2 ↑	97 ± 1 ↑	94 ± 2	96 ± 1 ↑	100 ± 0 ↑	99 ± 0 ↑	95 ± 2
C. aquatilis	89 ± 1	88 ± 7 ↑	90 ± 3 ↑	95 ± 2 ↑	98 ± 0 ↑	98 ± 0	95 ± 0 ↑	93 ± 1 ↑	97 ± 1 ↑	94 ± 2
C. utriculata[*,a]	93 ± 2	97 ± 1 ↑	96 ± 2 ↑	99 ± 1 ↑	90 ± 5 ↑	83 ± 1	91 ± 3 ↑	97 ± 1 ↑	99 ± 1 ↑	94 ± 2
J. torreyi	94 ± 1	95 ± 3 ↑	94 ± 2 ↑	96 ± 0 ↑	90 ± 2 ↑	92 ± 6	93 ± 2 ↑	97 ± 2 ↑	91 ± 2 ↑	94 ± 1
J. arcticus	89 ± 0	90 ± 6 ↑	89 ± 4 ↑	96 ± 0 ↑	97 ± 2 ↑	96 ± 4	94 ± 0 ↑	91 ± 3 ↑	96 ± 2 ↑	93 ± 2
C. microptera	80 ± 6 ↓	88 ± 8 ↑	83 ± 4 ↑	93 ± 3 ↑	92 ± 4 ↑	82 ± 3	82 ± 4 ↑	93 ± 3 ↑	96 ± 3 ↑	88 ± 2
P. arundinacea[*]	92 ± 1	81 ± 4 ↑	87 ± 1 ↑	89 ± 1 ↑	65 ± 3	79 ± 4	90 ± 4 ↑	88 ± 2 ↑	92 ± 4 ↑	85 ± 3
T. latifolia	79 ± 6 ↓	81 ± 6 ↑	83 ± 6 ↑	83 ± 3 ↑	85 ± 4 ↑	89 ± 4	84 ± 1 ↑	90 ± 2 ↑	92 ± 2 ↑	85 ± 2
C. canadensis	90 ± 1	65 ± 6	73 ± 11	80 ± 4 ↑	69 ± 2	94 ± 4	82 ± 2 ↑	78 ± 2 ↑	85 ± 2 ↑	80 ± 4
H. jubatum	76 ± 1 ↓	66 ± 5	71 ± 3	88 ± 4 ↑	88 ± 7 ↑	86 ± 4	87 ± 5 ↑	80 ± 4 ↑	79 ± 1 ↑	80 ± 2
P. vulgaris	81 ± 11	87 ± 6 ↑	87 ± 1 ↑	84 ± 4 ↑	62 ± 5	77 ± 8	75 ± 1	82 ± 2 ↑	74 ± 2	79 ± 3
P. virgatum[*]	70 ± 6 ↓	69 ± 4	66 ± 3	81 ± 5 ↑	75 ± 4	92 ± 2	77 ± 6 ↑	83 ± 3 ↑	71 ± 3	76 ± 3
P. australis	53 ± 2 ↓	65 ± 5	67 ± 5	73 ± 3	88 ± 5 ↑	67 ± 6 ↓	79 ± 2 ↑	87 ± 4 ↑	89 ± 1 ↑	74 ± 3
I. missouriensis	83 ± 6	63 ± 4	67 ± 5	83 ± 2 ↑	70 ± 4	92 ± 1	69 ± 2	69 ± 0	67 ± 3	74 ± 3
L. cinereus[*]	66 ± 5 ↓	62 ± 5	69 ± 2	61 ± 3	69 ± 3	79 ± 2	74 ± 1	77 ± 3 ↑	72 ± 1	70 ± 2
Control[*]	92 ± 1	62 ± 4	58 ± 1	65 ± 9	66 ± 1	88 ± 2	69 ± 2	64 ± 1	66 ± 2	70 ± 3

[a] COD removal differed significantly between 4 °C and 24 °C in treatments with an asterisk.
[b] Within each column, values followed by (↑) had significantly higher COD removal than the control; values followed (↓) by had significantly lower COD removal than the control ($p < 0.05$, planned contrast within ANOVA).
[c] Treatments are sorted in descending order of study-long average COD removal calculated as the mean of all nine batches.
[*] Repeated measures ANOVA ($p < 0.05$).

In another study, Du et al. (2018) analyzed the performance of an Integrated Vertical-Flow Constructed Wetlands (IVCWs) in removing nitrogen for treating water.
Four sets of lab-scale IVCWs were built with a 25 L working volume. Natural sands (in the same diameter 1–2 mm) were filled into each tank as the substrate layers (35 cm). Arundo donax (A. donax), Canna indica L. (C. indica L.) and Acorus calamus L. (A. calamus L.) were selected as wetland vegetation, and which with the nearby biomass were planted in 3 sets of wetland system sequentially.
Results showed that IVCWs planted with vegetation generally achieved a higher Total Nitrogen removal rate than unplanted treatment, especially for *Canna indica L.* with 10.35% enhancement. The average N uptake rate was calculated in the order of *C. indica L. > A. donax > A. calamus L.*, for 22.88 mgN/m^3 /d, 18.21 mgN/m^3 /d and 16.68 mgN/m^3 /d, respectively.
Moreover, the microbial process proportion (83.87–87.94%) is the main Nitrogen removal pathway in IVCW, and vegetation planting could increase 8.16% of it in average. The average NO3-N removal rates of 95.2%, 97.2%, 96.8% and 96.2% occurred in summer (Aug. and Sep.), while 83.3%, 84.4%, 77.56% and 73.45% in autumn (Oct. to Dec.).

In China, Song et al. (2006) observed the seasonal efficiency of a constructed wetland for sewage treatment. The wetland has a total area of 80 ha and treatment capability of 2.0 × 104 m^3 d^{-1}. Average seasonal temperatures for the region are winter (from December to February) −0.1 ◦C, spring (from March to May) 11.1 ◦C, summer (from June to August) 22.9 ◦C and fall (from September to November) 14.6 ◦C (2003 data).
Results (Removal): SS (71.8 ± 8.4%), BOD5 (70.4 ± 9.6%), COD (62.2 ± 10.1%), total coliform (99.7%), fecal coliform (99.6%), ammonia nitrogen was relatively low (40.6 ± 15.3%), and total phosphorus showed the least efficient reduction (29.6 ± 12.8%). Mean percent reduction was higher during spring (72.8%) and summer (74.1%) and lower during autumn (66.6%) and winter (67.8%)

Kadlec and Reddy (2001) did a literature review of the impact of change in temperature on treatment efficiency of wetlands. The temperature coefficient (Θ) varied from 1.05 to 1.37 for carbon and nitrogen cycling processes during isolated conditions. Phosphorus sorption reactions are least affected by temperature, with Θ values of 1.03 to 1.12. Temperature seems to have minimal effect on biochemical oxygen demand ($0.900 < \Theta < 1.015$) and phosphorus ($0.995 < \Theta < 1.020$) removal, and more significant effect on nitrogen removal ($0.988 < \Theta < 1.16$). See all results tables for more precise details on each result for each reference and also look beneath in the methodology for some insight on an equation description.

Land et al. (2016) focused on the efficiency of recreated wetlands in nitrogen and phosphorous removal. They did an analysis based on many other studies results, mainly studies across Europe and the US. Median removal rates of nitrogen and phosphorous were 93 and 1.2 g m^{-2} $year^{-1}$, respectively. Removal efficiency for Total Nitrogen was significantly correlated with hydrologic loading rate (HLR) and Temperature, and the median was 37 %, with a 95 % confidence interval of 29–44 %. Removal efficiency for Total Phosphorous was significantly correlated with inlet Total Phosphorous concentration, HLR, Temperatures, and Average Median Total Phosphorous removal efficiency was 46 % with a 95 % confidence interval of 37–55 %. Maximum in removal efficiency appeared at intermediate annual average temperatures (approximately 14–19 °C). For nitrogen we have a table per climate region (Aw, Cfa, Cfb, Csa, Dfa, Dfb):

Figure 2 – Removal efficiency depending on regional climate characteristics

	n[a]	Ln R ± 1 SE	R	Median removal efficiency (%)	95 % confidence interval
All wetlands	38	−0.46 ± 0.05	0.63	37	29–43
Climate zone					
Aw (equatorial savannah, dry winter)	1	−0.49 ± 0.21	0.61	39	7–60
Cfa (warm, fully humid, hot summer)	6	−0.47 ± 0.15	0.63	37	15–54
Cfb (warm, fully humid, warm summer)	19	−0.44 ± 0.08	0.64	36	23–46
Csa (warm, dry and hot summer)	3	−0.63 ± 0.02	0.53	47	44–50
Dfa (snow, fully humid, hot summer)	5	−0.61 ± 0.12	0.54	46	30–58
Dfb (Snow, fully humid, warm summer)	4	−0.31 ± 0.11	0.73	27	9–42

In Sweden Valkama et al. (2017) indicate that the mean temperature in 2014 was 6.2◦C and precipitation 320 mm. Normal annual mean temperatures in this boreal region is 5.0 ◦C and annual precipitation is 660 mm. The coldest month was January (mean temperature −7.5 ◦C) and warmest July (mean temperature 19.1 ◦C).
The incoming and outgoing TP and NO_3–N loads were calculated and the relative and absolute reduction rates were determined.
The wetland received 24 g P m^{-2} $year^{-1}$ and 130 g NO3–N m^{-2} $year^{-1}$ and it retained 3.1 g m^{-2} $year^{-1}$ of P and 18 g m^{-2} $year^{-1}$ of NO3–N. Annual TP reduction was 13% and NO3–N reduction 14%. The monthly relative NO_3–N reduction was 25–82% in growing season (June–September), 7–10% in January–March and 4–6% in November–December. The highest absolute monthly reduction of NO_3–N occurred in December

- **Methodology**

- Method 1 Georgi and Zafiriadis (2006)

In a study in Greece, the authors used Thom's discomfort index for population based on air temperature and relative humidity in order to justify the use of vegetation in mitigating solar radiation and air temperatures (equations for temperature and radiation relative impact on vegetation also available):

$$DI = TEM - 0.55\,(1 - 0.01\,HUM)\,(TEM - 14.5)\ ^{\circ}\mathrm{C}$$

where:

DI = Discomfort Index in °C (DI)
TEM = Air temperature °C.
HUM = Relative humidity (percentage) %.

<21 degrees = no discomfort / 21-24 = under 50% population feels discomfort / 24-27 = most 50% population feels discomfort / 27-29 = Most population suffers discomfort / 29-32 = everyone feels severe stress / >32 = state of medical emergency.

- Method 2 (Kadlec & Reddy, 2001)

Areal removal rate:

$$k = k_{20}\theta^{(T-20)}$$

$$k_V = k_{V20}\theta^{(T-20)}$$

Where k_{20} = areal removal rate constant at 20 °C (m/a); k_{V20} = volumetric removal rate constant at 20 °C (1/d); T = temperature (°C); Θ = temperature

Another descriptor in the literature is Q_{10}, which measures the effect of a 10 °C change in temperature and is defined as the ratio of removal rates:

$$Q_{10} = \frac{\text{Rate at } (T + 10)}{\text{Rate at } T} = \theta^{10}$$

If Θ = 1.072, then a 10 °C temperature increase will double the value of the rate constant (Q_{10} = 2). If the value of u is less than unity, then the removal process slows with increasing temperature

Manoli et al. (2019)Urban Heat Island explained (methodology) by air temperature, albedo among others.

2.2 Integration of literature review with the CDS datasets

See section 1.2 for a general instruction

Datasets:

- ERA5 monthly data on single level
- CMIP5 monthly data on single level

Indicators created:

- **Air temperature**
  - Units: degrees Celsius
  - Frequency: monthly
  - ERA5 variable: “2 m temperature”
  - CMIP5 variable: “2 m temperature“
  - Note: original units in Kelvin
- **Monthly precipitation**:
  - Units: mm per month
  - ERA5 variable: “Mean total precipitation rate”
  - CMIP5 variable: “Mean precipitation flux“
  - Note: original units in mm/s

2.3 Integration of climate indicators into the SAVi natural infrastructure model

Natural infrastructure related indicators developed for and extracted from the CDS toolbox include impacts on rainwater harvesting and flood risk, climate impacts on nutrient absorption in NI assets and vegetation impacts on temperature. The CLD representing the dynamics of the SAVi Natural Infrastructure model is presented in is presented in Figure 55.

Figure 3 Causal Loop Diagram for natural infrastructure - CDS variables included

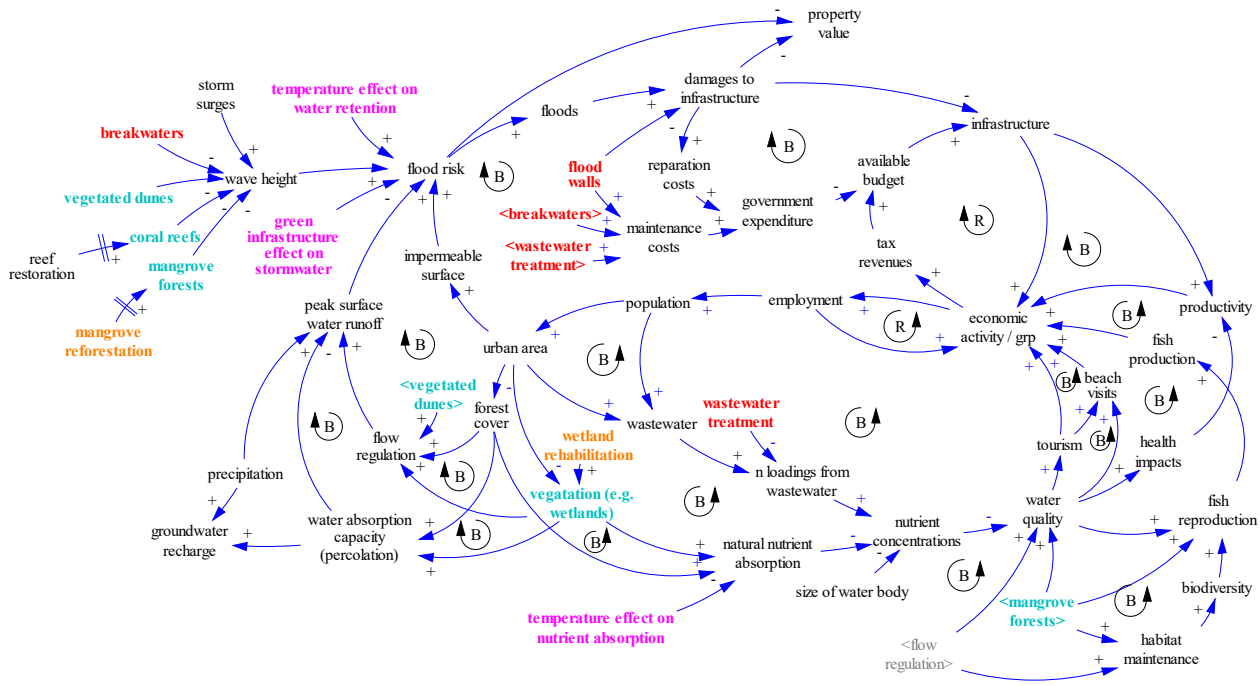

Flood risk is estimated as a function of temperature area and permeability, peak surface water runoff. The CDS indicator “effect of temperature on water retention” refers to the ability of natural landscapes to retain water given a specific outside temperature. The “effect of green infrastructure on stormwater” refers to potential reductions in stormwater runoff through the implementation of NBI assets (i.e. vegetation). The implementation of green roofs, vegetation strips and riparian buffers increases water retention on built assets and hence reduces flood risk by reducing peak stormwater flows during precipitation events.

The impact of temperature on nutrient absorption of natural infrastructure developed for the CDS toolbox refers to changes in the rate at which NI removes nutrients such as nitrogen and phosphorus. Nutrient absorption in NI assets such as wetlands highly depends on the type of vegetation and climatic conditions.

2.4 Behavioral impacts resulting from the integration of climate variables

Using the CDS toolbox to forecast the flood mitigation capacity of NI allows to capture the seasonality of ecosystem service provisioning for simulating seasonal severity of flood damages in the SAVi simulations. The use of this indicator improves the forecasting of future flood risk and damages, and increases the accuracy of NI’s contribution to flood mitigation given a range of climate scenarios. This will affect the return on investment of NI assets by changing flood damages incurred, depending on whether the NI asset is located in favorable or unfavorable climatic conditions.

The impacts of green infrastructure on stormwater runoff developed for and extracted from the CDS toolbox affects total peak stormwater runoff and stormwater related management costs as well as flood risk during stormwater events. An increase in the capacity of urban areas to store rainwater and delay runoff hence leads to a reduction in total stormwater loads, which translates into reduced costs of stormwater management. As water is retained and released over time, NI and NBI contribute to reducing flood risk and reduce flood damages incurred in areas with improved absorption and infiltration capacity.

Nutrient absorption is an essential service provided by NI, especially wetlands and riparian buffers. The use of the CDS indicator forecasting climate change impacts on nutrient absorption of NI in the SAVi model has far reaching impacts on various aspects of the model and simulation results. Changes in nutrient absorption affects the asset's capacity to remove nutrients from water stored with impacts on ecosystem service delivery, the value of ecosystem services provided and water quality. By impacting water quality, nutrient concentration further affects indicators such as chlorophyll-a concentration, water clarity, and the valuation of economic activities such as fisheries, tourism and real estate.

2.5 Simulation results

With regard to SAVi Natural Infrastructure, different variables were developed using the CDS database. Natural infrastructure both is impacted by its surrounding climatic conditions as well as impacts its surrounding environment in various ways. An example of the former is the impact of temperature on phosphorus (P) removal efficiency in wetlands. An example of the latter is the use of trees and urban green infrastructure to reduce the heat island effect. The following three variables were developed to incorporate data from the CDS toolbox: (1) Effect of temperature on P removal efficiency in wetlands, (2) effect of vegetation cover on surrounding temperature, and (3) the number of months during which heat impacts on health can occur.

2.5.1 Effect of temperature on P removal efficiency in wetlands

El-Rafaie (2010) describes the impact of temperature on the removal efficiency of the Manzala Engineerede Wetland in Egypt. The results of the study indicate that the P removal efficiency of wetland increases with temperature. The following equation is used to forecast the P removal efficiency of wetlands using CDS data:

*P removal efficiency of wetlands = (1.4035 * seasonal temperature - 10.888) / 100*

Forecasting P removal efficiency in wetlands allows to estimate the value of nutrient removal in relation to local climatic conditions. Figure 56 presents the results for the BAU (red line) and the CDS climate impact scenario (blue line) respectively.

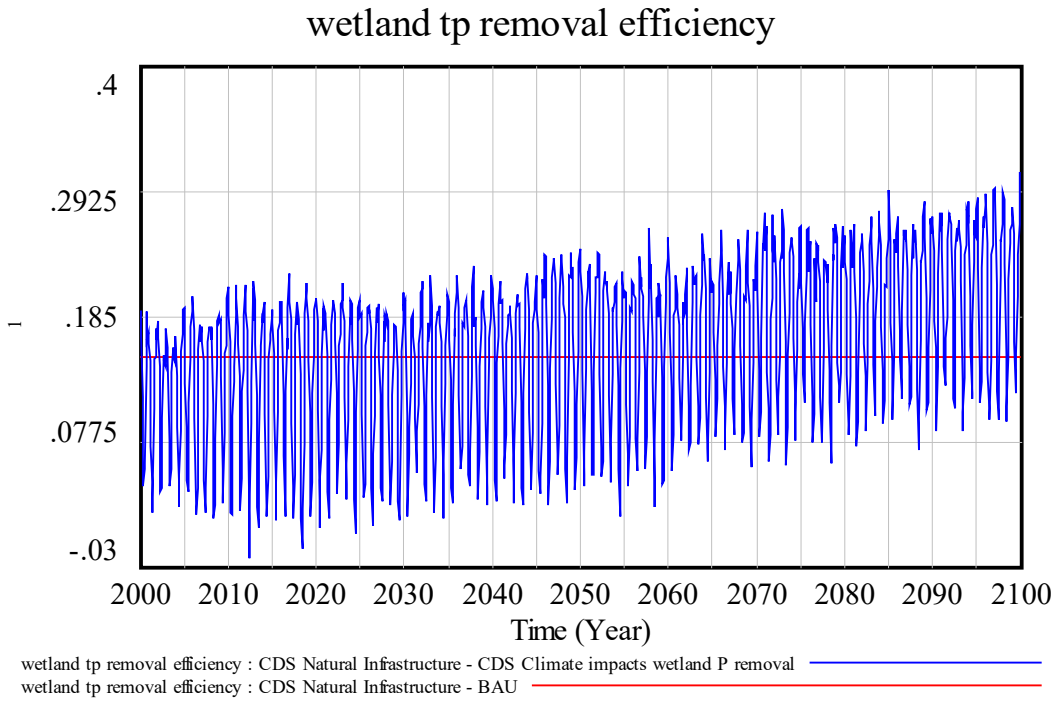

Figure 4: P removal efficiency in wetlands

The graph above illustrates that the overall removal efficiency of wetlands is projected to increase in the area around Johannesburg, due to the projected increase in temperature in the IPSL RCP8.5 scenario. The seasonal fluctuation of P removal efficiency directly affects water quality of waterbodies that receive the effluent of the wetland. Figure 57 illustrates the P loadings in wetland effluent (water leaving the wetland) and how the constant formulation in the BAU scenario significantly underestimates P loadings from wetland effluent.

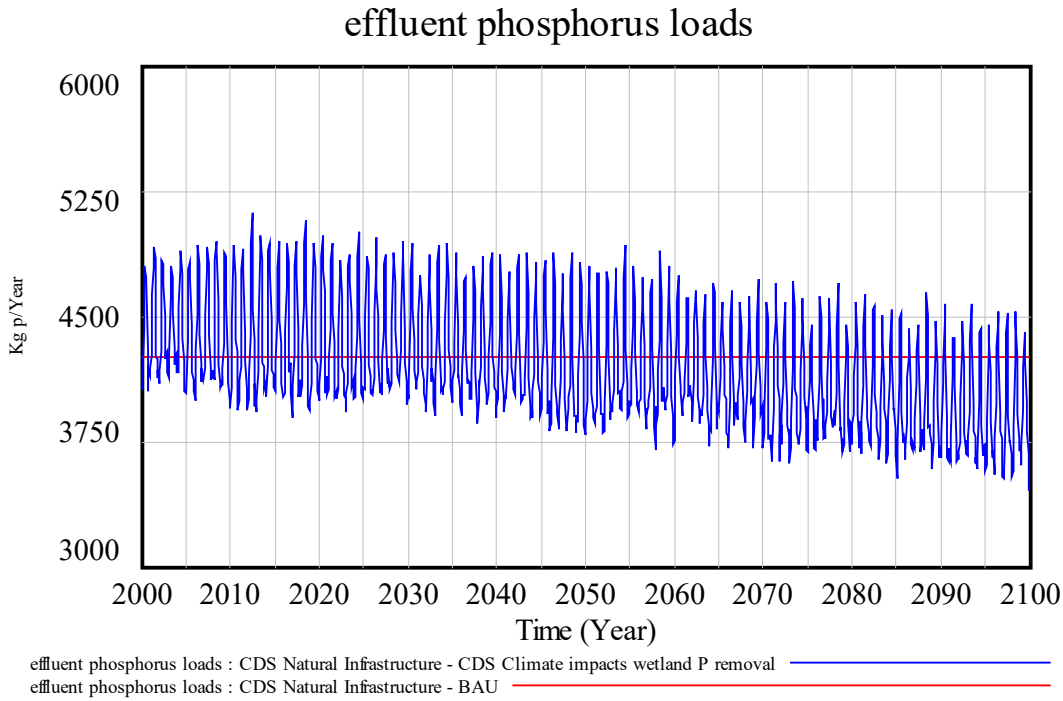

Figure 5: Wetland effluent phosphorus loads

Cumulatively, the amount of P removed by the wetland is 60.06 ton P and 67.29 ton P in the no impact and CDS climate impact scenario respectively. This is equivalent to an annual reduction of 750.58 kg P (no impact scenario) and 841.13 kg P (CDS climate impact scenario) per year respectively. Assuming an average cost of P removal in wastewater treatment plants of USD 68.38 per kg P removed, the cumulative avoided cost of wastewater treatment between 2020 and 2100 total USD 4.11 million in the no impact scenario and USD 4.60 million in the CDS impact scenario. Both the amount of P removed and related cost in the CDS impact scenario are 12% higher compared to the no impact scenario.

2.5.2 Effect of temperature on labor productivity and impacts of vegetation cover

We have assumed that working in temperatures above 25 degree Celsius exposes individuals to a higher risk of suffering adverse health impacts, leading to higher health cost and the need for replacement workers. The CDS climate data is used to forecast the number of months during which adverse health impacts may occur. The following equation is used to calculate the labor productivity impact indicator:

Labor productivity impact indicator = IF THEN ELSE (Tair>25, Tair / 25, 0)

The IF THEN ELSE function assesses whether the threshold temperature (25) is exceeded and hence whether impacts may occur. Dividing air temperature by the threshold value indicates the potential strength of impacts relative to the threshold temperature. Figure 58 presents the forecasted labor productivity impact indicator for Johannesburg

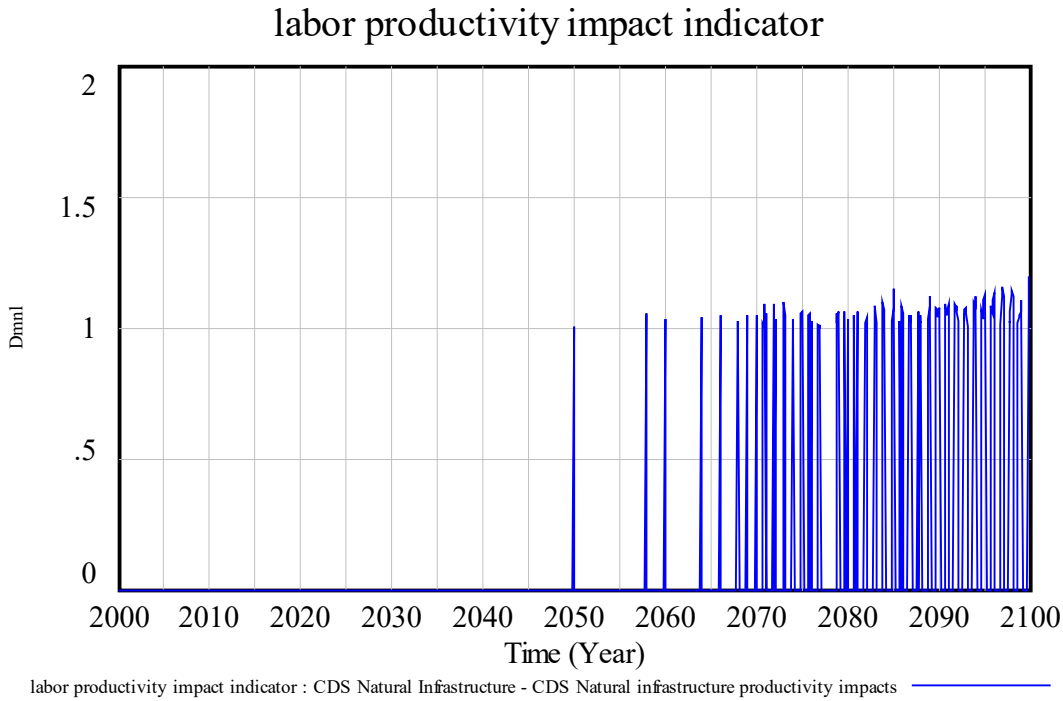

Figure 6: Labor productivity impact indicator

The forecast indicates that temperature related labor productivity impacts start occurring around the year 2050/2060 and become frequent after 2065.

2.5.3 Impacts of vegetation cover on surrounding air temperature

The literature review above has highlighted the role of trees and green spaces for temperature regulation in urban environments. Vegetation cover mitigates sun radiation and provides shade and hence contributes to counteracting the urban heat island effect. The average reduction for a 25% increase in vegetation cover is 1.635 °C.

In light of the temperature-related labor productivity impacts described above, three indicators were developed for assessing potential benefits of increasing vegetation cover in Johannesburg. Table 21 provides an overview of the three indicators and their equations

Indicator	Equation
Air temperature 25% vegetation cover	= Tair – 1.635
Air temperature 50% vegetation cover	= Tair – 3.27
Air temperature 75% vegetation cover	= Tair – 4.905

Table 2: Air temperature indicators considering vegetation cover

Assuming the same temperature threshold for the occurrence of temperature related impacts on labor productivity (25 degree Celsius), the labor productivity impact indicator is simulated using

the three different air temperature values. This simulation assumes that the vegetation cover in Johannesburg is close to 0%, for illustration purposes.

The results for the simulations using different CDS based air temperature values are presented in Figure 59. The figure in the top left represents the simulation without vegetation cover, as already presented in Figure 58. The subsequent figures represent the months with potential labor productivity impacts considering 25% (top right), 50% (bottom left) and 75% (bottom right) vegetation cover.

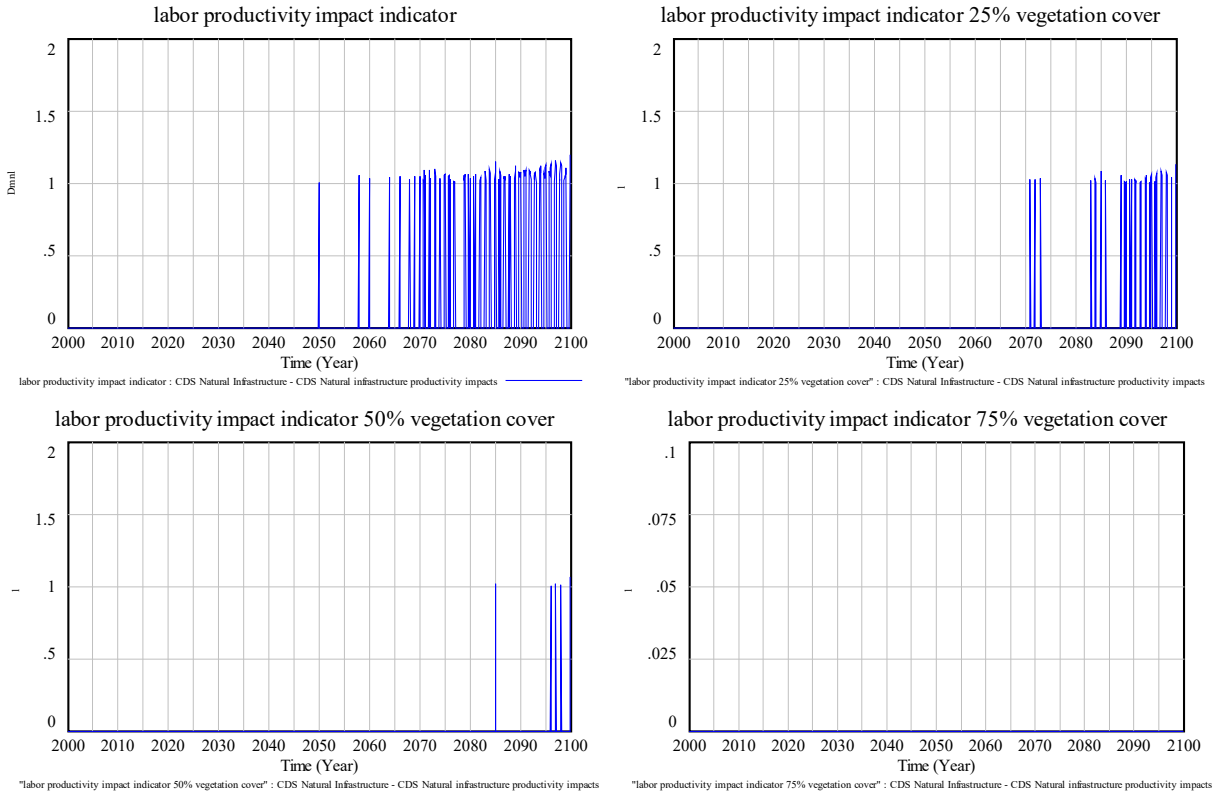

Figure 7: Labor productivity impact indicator and the impacts of vegetation cover

The results illustrate that increasing vegetation cover in the form of trees and green roofs could postpone the onset of temperature related impacts on labor productivity, or even mitigate it entirely (75% vegetation cover).

3 Bibliography

Acclimatise. (2009). *Building Business Resilience to Inevitable Climate Change. Carbon Disclosure Project Report. Global Electric Utilities.* Oxford.

Adeh, E. H., Good, S. P., Calaf, M., & Higgins, C. W. (2019). Solar PV Power Potential is Greatest Over Croplands. *Scientific reports, vol(9), no(1)*, pp. 1-6.

Ahsan, S., Rahman, M. A., Kaneco, S., Katsumata, H., Suzuki, T., & Ohta, K. (2005). Effect of temperature on wastewater treatment with natural and waste materials. *Clean Technologies and Environmental Policy, 7(3)*, 198-202.

Akbari, H. (2005). *Energy saving potentials and air quality benefits of urban heat island mitigation.* Récupéré sur OSTI.org: https://www.osti.gov/biblio/860475/

Akbari, H., Davis, S., Dorsano, S., Huang, J., & Winnett, S. (1992). *Cooling our communities: A guidebook on tree planting and light-colored surfacing.* Washington, DC (United States): Lawrence Berkeley Lab.; Environmental Protection Agency.

Alam, T., Mahmoud, A., Jones, K. D., Bezares-Cruz, J. C., & Guerrero, J. (2019). A Comparison of Three Types of Permeable Pavements for Urban Runoff Mitigation in the Semi-Arid South Texas, USA. *MDPI - Water, 11(10)*.

Allen, R. G., Pereira, L. S., Raes, D., & Smith, M. (2006). *FAO Irrigation and Drainage Paper - Crop Evapotranspiration.* FAO.

Allos, M. (2016, Juin). *Potential Damage Caused by Direct Lightning Strikes*. Récupéré sur Sollatek: https://www.sollatek.com/potential-damage-caused-direct-lightning-strikes/

American Society of Landscape Architects. (2003). *Chicago City Hall Green Roof*. Récupéré sur asla.org: http://www.asla.org/meetings/awards/awds02/chicagocityhall.html

Asian Development Bank. (2012). *Adaptation to Climate Change - The Case of a Combined Cycle Power Plant.* Philippines.

Attia, S. I. (2015). The influence of condenser cooling water temperature on the thermal efficiency of a nuclear power plant. *Annals of Nuclear Energy*, 371-378.

Bartos, M., Chester, M., Johnson, N., Gorman, B., Eisenberg, D., Linkov, I., & Bates, M. (2016). Impacts of rising air temperatures on electric transmission ampacity and peak electricity load in the United States. *Environmental Research Letters, 11(11), 1*.

Basha, M., Shaahid, S. M., & Al-Hadhrami, L. (2011). Impact of fuels on performance and efficiency of gas turbine power plants. *2nd International Conference on Advances in Energy Engineering*, (pp. 558-565). Bangkok.

Bassi, A. M., Pallaske, G., Wuennenberg, L., Graces, L., & Silber, L. (2019, March). *Sustainable Asset Valuation Tool: Natural Infrastructure.* Récupéré sur International Institute for Sustainable Development : https://www.iisd.org/sites/default/files/publications/sustainable-asset-valuation-tool-natural-infrastructure.pdf

Bengtson, H. (2020). *The Rational Method for Estimation of Design Surface Runoff Rate for Storm Water Control*. Récupéré sur brighthubengineering.com: https://www.brighthubengineering.com/hydraulics-civil-engineering/60842-the-rational-method-for-calculation-of-peak-storm-water-runoff-rate/

Bergel-Hayat, R., Debbarh, M., Antoniou, C., & Yannis, G. (2013). Explaining the road accident risk: weather effects. *Accident Analysis & Prevention, 60*, 456-465.

Berghage, R. D., Beattie, D., Jarrett, A. R., Thuring, C., Razaei, F., & O'Connor, T. P. (2009). *Green Roofs For Stormwater Runoff Control.* Cincinnati: EPA.

Bhatt, S., & Rajkumar, N. (2015). Effect of moisture in coal on station heat rate and fuel cost for Indian thermal power plants. *Power Research, 11(4)*, 773-786.

Bhattacharya, C., & Sengupta, B. (2016). Effect of ambient air temperature on the performance of regenerative air preheater of pulverised coal fired boilers. *Int. J. Energy Technology and Policy, Vol. 12, No. 2*, pp. 136–153.

Biswas, B. (2014). Construction and Evaluation of Rainwater Harvesting System for Domestic Use in a Remote and Rural Area of Khulna, Bangladesh. *International Scholarly Research Notices*. doi:https://doi.org/10.1155/2014/751952

Brouwer, C., & Heibloem, M. (1986). Irrigation Water Management and Irrigation Water Needs. *FAO - Training manual, 3.*

Brouwer, C., Prins, K., & Heibloem, M. (1989). *Irrigation water management: irrigation scheduling.* Récupéré sur Fao.org: http://www.fao.org/3/T7202E/t7202e00.htm#Contents

Büyükalaca, O., Bulut, H., & Yılmaz, T. (2001). Analysis of variable-base heating and cooling degree-days for Turkey. *Applied Energy, 69(4)*, pp. 269-283.

Carnegie Mellon University (CMU). (s.d.). *Integrated Environmental Control Model.* Récupéré sur Department of Engineering & Public Policy (EPP): https://www.cmu.edu/epp/iecm/

Chinowsky, P. S., Price, J. C., & Neumann, J. E. (2013). Assessment of climate change adaptation costs for the US road network. *Global Environmental Change, 23(4)*, 764-773.

Chinowsky, P., Hayles, C., Schweikert, A., Strzepek, N., Strzepek, K., & Schlosser, A. (2011). Climate change: comparative impact on developing and developed countries. *The Engineering Project Organization Journal*, pp. 67-80.

Choi, T., Keith, L., Hocking, E., Friedman, K., & Matheu, E. (2011). *Dams and energy sectors interdependency study.*

City of Chicago Department of Environment. (2006). *Green roof test plot project: annual project summary report.* Chicago.

Colman, J. (2013, Avril 26). The effect of ambient air and water temperature on power plant efficiency. *Master Thesis*. Duke University Libraries.

Cronshey, R., McCuen, R. H., Miller, N., Rawls, W., Robbins, S., & Woodward, D. (1986, June). *Urban Hydrology for Small Watersheds.* Récupéré sur USDA-United States Department of Agriculture: https://www.nrcs.usda.gov/Internet/FSE_DOCUMENTS/stelprdb1044171.pdf

Das, T. K., Saharawat, Y. S., Bhattacharyya, R., Sudhishri, S., Bandyopadhyay, K. K., Sharma, A. R., & Jat, M. L. (2018). Conservation agriculture effects on crop and water productivity, profitability and soil organic carbon accumulation under a maize-wheat cropping system in the North-western Indo-Gangetic Plains. *Field Crops Research, 215*, pp. 222-231.

Davies, Z. G., Edmondson, J. L., Heinemeyer, A., Leake, J. R., & Gaston, K. J. (2011). Mapping an urban ecosystem service: quantifying above-ground carbon storage at a city-wide scale. *Journal of applied ecology, 48(5)*, pp. 1125-1134.

Davy, R., Gnatiuk, N., Pettersson, L., & Bobylev, L. (2018). Climate change impacts on wind energy potential in the European domain with a focus on the Black Sea. *Renewable and sustainable energy reviews*, pp. 1652-1659.

De Oliveira, V., De Mello, C., Viola, M., & Srinivasan, R. (2017). Assessment of climate change impacts on the streamflow and hydropower potential in the headwater region of the

Grande river basin, Southeastern Brazil. *International Journal of Climatology 37[15]*, pp. 5005-5023.

De Rosa, M., Bianco, V., Scarpa, F., & Tagliafico, L. A. (2014). Heating and cooling building energy demand evaluation; a simplified model and a modified degree days approach. *Applied Energy, 128*, 217-229.

De Sa, A., & Al Zubaidy, S. (2011). Gas turbine performance at varying ambient temperature. *Applied Thermal Engineering, 31(14-15)*, 2735-2739.

Demuzere, M., Orru, K., Heidrich, O., Olazabal, E., Geneletti, D., Orru, H., . . . Faehnle, M. (2014). Mitigating and adapting to climate change: Multi-functional and multi-scale assessment of green urban infrastructure. *Journal of environmental management, 146*, pp. 107-115.

Dhakal, S., & Hanaki, K. (2002). Improvement of urban thermal environment by managing heat discharge sources and surface modification in Tokyo. *Energy and buildings, 34(1)*, pp. 13-23.

Diaz, C. A., Osmond, P., & King, S. (2015). Precipitation and buildings: estimation of the natural potential of locations to sustain indirect evaporative cooling strategies through hot seasons. *Living and Learning: Research for a Better Built Environment: 49th International Conference of the Architectural Science Association*, (pp. 45-54). Melbourne.

Djaman, K., O'Neill, M., Owen, C. K., Smeal, D., Koudahe, K., West, M., & Irmak, S. (2018). Crop evapotranspiration, irrigation water requirement and water productivity of maize from meteorological data under semiarid climate. *MDPI - Water 2018, 10(4), 405*.

Doorenbos, J., & Kassam, A. (1979). *Yield response to Water Irrigation and Drainage.* Roma: Food and Agricultural Organization; Paper No 33.

Drax. (2017, August 29). *Technology - What hot weather means for electricity*. Récupéré sur Drax.com: https://www.drax.com/technology/hot-weather-means-electricity/

Du, L., Trinh, X., Chen, Q., Wang, C., Wang, H., Xia, X., . . . Wu, Z. (2018). Enhancement of microbial nitrogen removal pathway by vegetation in Integrated Vertical-Flow Constructed Wetlands (IVCWs) for treating reclaimed water. *Bioresource technology, 2*.

Dunn, A. D. (2007). *Green light for green infrastructure.* Récupéré sur Digitalcommons.pace.edu: https://digitalcommons.pace.edu/lawfaculty/494

Durmayaz, A., & Sogut, O. S. (2006). Influence of cooling water temperature on the efficiency of a pressurized-water reactor nuclear-power plant. *International Journal of Energy Research, 30(10)*, pp. 799-810.

East Coast Lightning Equipment INC. (s.d.). *Lightning protection installation cost study* . Récupéré sur East Coast Lightning Equipment INC: https://ecle.biz/coststudy/

Eliasson, J., & Ludvigsson, G. (2000). Load factor of hydropower plants and its importance in planning and design. *11th International Seminar on Hydro Power Plants.* Vienna.

El-Refaie, G. (2010). Temperature impact on operation and performance of Lake. *Ain Shams Engineering Journal 1*, 1-9.

El-Shobokshy, M. S., & Hussein, F. M. (1993). Degradation of photovoltaic cell performance due to dust deposition on to its surface. *Renewable Energy, 3(6-7)*, pp. 585-590.

Engineering ToolBox. (2009). *Pumping Water - Energy Cost Calculator*. Récupéré sur engineeringtoolbox.com: https://www.engineeringtoolbox.com/water-pumping-costs-d_1527.html

Engineering ToolBox. (s.d.). *Hydropower*. Récupéré sur Engineering ToolBox: https://www.engineeringtoolbox.com/hydropower-d_1359.html

EPA. (2014). *The Economic Benefits of Green Infrastructure - A Case Study of Lancaster, PA.*

Eurostat. (2019). *Energy statistics - cooling and heating degree days (nrg_chdd)*. Récupéré sur Eurostat, the Statistical Office of the European Union: https://ec.europa.eu/eurostat/cache/metadata/en/nrg_chdd_esms.htm

Eurostat, the Statistical Office of the European Union. (2019). *Energy statistics - cooling and heating degree days (nrg_chdd)*. Récupéré sur Europa.eu: https://ec.europa.eu/eurostat/cache/metadata/en/nrg_chdd_esms.htm

Evans, D. V., & Antonio, F. D. (1986). Hydrodynamics of Ocean Wave-Energy Utilization: IUTAM Symposium Lisbon/Portugal 1985. *Springer Science & Business Media*, pp. 133-156.

Farkas, Z. (2011). *Considering air density in wind power production.* Budapest.

Fisher, J. C., Bartolino, J. R., Wylie, A. H., Sukow, J., & McVay, M. (2016). *Groundwater-flow model for the Wood River Valley aquifer system, south-central Idaho.* US Geological Survey.

Flowers, M. E., Smith, M. K., Parsekian, A. W., Boyuk, D. S., McGrath, J. K., & Yates, L. (2016). Climate impacts on the cost of solar energy. *Energy Policy, 94*, pp. 264-273.

Gajbhiye, S., Mishra, S. K., & Pandey, A. (2013). Effects of Seasonal/Monthly Variation on Runoff Curve Number for Selected Watersheds of Narmada Basin. *International Journal of Environmental Sciences, Volume 3, No 6*, pp. 2019-2030.

Garfí, M., Pedescoll, A., Bécares, E., Hijosa-Valsero, M., Sidrach-Cardona, R., & García, J. (2012). Effect of climatic conditions, season and wastewater quality on contaminant removal efficiency of two experimental constructed wetlands in different regions of Spain. *Science of the total environment, 437*, pp. 61-67.

Georgi, N. J., & Zafiriadis, K. (2006). The impact of park trees on microclimate in urban areas. *Urban Ecosystems, 9(3)*, pp. 195-209.

Ghamami, M., Fayazi Barjin, A., & Behbahani, S. (2016). Performance Optimization of a Gas Turbine Power Plant Based on Energy and Exergy Analysis. *Mechanics, Materials Science & Engineering Journal, 29*.

GIZ. (2016). *Solar Powered Irrigation Systems (SPIS) – Technology, Economy, Impacts.* Récupéré sur Gesellschaft für Internationale Zusammenarbeit (GIZ): https://energypedia.info/images/temp/2/23/20160630122544!phpeKHVUr.pdf

Gomes, J., Diwan, L., Bernardo, R., & Karlsson, B. (2014). Minimizing the Impact of Shading at Oblique Solar Angles in a Fully Enclosed Asymmetric Concentrating PVT Collector. *Energy Procedia (57)*, pp. 2176-2185.

Good, E., & Calaf, S. (2019). Solar PV Power Potential is Greatest Over Croplands. *SciRep (9, 11442)*.

Green, A. (2020). *The intersection of energy and machine learning*. Récupéré sur adgefficiency.com: https://adgefficiency.com/energy-basics-ambient-temperature-impact-on-gas-turbine-performance/

Haerter, J., Hagemann, S., Moseley, C., & Piani, C. (2011). Climate model bias correction and the role of timescales. *Hydrology and Earth System Sciences, 15*, pp. 1065-1073.

Handayani, K., Filatova, T., & Krozer, Y. (2019). The Vulnerability of the Power Sector to Climate Variability and Change: Evidence from Indonesia. *Energies, 12(19), 3640*.

Harrison, G. P., & Whittington, H. W. (2002). Vulnerability of hydropower projects to climate change. *IEE proceedings-generation, transmission and distribution, 149(3)*, pp. 249-255.

Harrison, G., & Wallace, A. (2005). Climate sensitivity of marine energy. *Renewable Energy, 30(12)*, pp. 1801-1817.

Henry, C. L., & Pratson, L. F. (2016). Effects of environmental temperature change on the efficiency of coal-and natural gas-fired power plants. *Environmental science & technology, 50(17)*, 9764-9772.

Hutyra, L. R., Yoon, B., & Alberti, M. (2011). Terrestrial carbon stocks across a gradient of urbanization: a study of the Seattle, WA region. *Global Change Biology, 17(2)*, pp. 783-797.

Ibrahim, S., Ibrahim, M., & Attia, S. (2014). The impact of climate changes on the thermal performance of a proposed pressurized water reactor: nuclear-power plant. *International Journal of Nuclear Energy*.

Jabboury, B. G., & Darwish, M. A. (1990). Performance of gas turbine co-generation power desalting plants under varying operating conditions in Kuwait. *Heat Recovery Systems and CHP, 10(3)*, 243-253.

Jackson, N., & Puccinelli, J. (2006). *Long-Term Pavement Performance (LTPP) data analysis support: National pooled fund study TPF-5 (013)-effects of multiple freeze cycles and deep frost penetration on pavement performance and cost (No. FHWA-HRT-06-121).*

Janssen, H., Carmeliet, J., & Hens, H. (2004). The influence of soil moisture transfer on building heat loss via the ground. *Building and Environment, 39(7)*, 825-836.

Jerez, S., Tobin, I., Vautard, R., Montávez, J. P., López-Romero, J. M., Thais, F., . . . Wild, M. (2015). The impact of climate change on photovoltaic power generation in Europe. *Nature Communications, 6(1)*, pp. 1-8.

Ji, M., Hu, Z., Hou, C., Liu, H., Ngo, H. H., Guo, W., . . . Zhang, J. (2020). New insights for enhancing the performance of constructed wetlands at low temperatures. *Bioresource Technology, 122722*.

JICA. (March 2003). *Manual on flood control planning.* Department of public works and highways.

Jim, C. Y., & Chen, W. Y. (2008). Assessing the ecosystem service of air pollutant removal by urban trees in Guangzhou (China). *Journal of environmental management, 88(4)*, pp. 665-676.

Kadlec, R. H., & Reddy, K. R. (2001). Temperature effects in treatment wetlands. *Water environment research, 73(5)*, pp. 543-557.

Kakaras, E., Doukelis, A., Prelipceanu, A., & Karellas, S. (2006). Inlet air cooling methods for gas turbine based power plants.

Kaldellis, J., & Fragos, P. (2011). Ash deposition impact on the energy performance of photovoltaic generators. *Journal of cleaner production, 19(4)*, pp. 311-317.

Kappos, L., Ntouros, I., & Palivos, I. (1996). Pollution effect on PV system efficiency. *Proceedings of the 5th National Conference on Soft Energy Forms.* Athens.

Kivi, R. (2017, Avril 24). *How Does Geothermal Energy Work?* Récupéré sur Sciencing: https://sciencing.com/geothermal-energy-work-4564716.html

Kloss, C., & Calarusse, C. (2011). *Rooftops to Rivers: Green strategies for controlling stormwater and combined sewer overflows.* New-York.

Koc, C. B., Osmond, P., & Peters, A. (2018). Evaluating the cooling effects of green infrastructure: A systematic review of methods, indicators and data sources. *Solar Energy, 166*, pp. 486-508.

Koch, H., & Vögele, S. (2009). Dynamic modelling of water demand, water availability and adaptation strategies for power plants to global change. *Ecological Economics, 68(7)*, pp. 2031-2039.

Kosa, P. (2011). The effect of temperature on actual evapotranspiration based on Landsat 5 TM Satellite Imagery. *Evapotranspiration, 56(56)*, pp. 209-228.

Krishna, P., Kumar, K., & Bhandari, N. M. (2002). IS: 875 (Part3): Wind loads on buildings and structures-proposed draft & commentary. Document No.: IITK-GSDMA-Wind, 02-V5. Roorkee, Uttarakhand, India: Department of Civil Engineering; Indian Institute of Technology Roorkee.

Kumpulainen, L., Laaksonen, H., Komulainen, R., Martikainen, A., Lehtonen, M., Heine, P., . . . Saaristo, H. (2007). *Distribution Network 2030 - Vision of the future power system.* Finland: VTT.

Land, M., Granéli, W., Grimvall, A., Hoffmann, C. C., Mitsch, W. J., Tonderski, K. S., & Verhoeven, J. T. (2016). How effective are created or restored freshwater wetlands for nitrogen and phosphorus removal? A systematic review. *Environmental Evidence, 5*.

Larsen, P., Goldsmith, S., Wilson, M., Strzepek, K., Chinowsky, P., & Saylor, B. (2008). Estimating future costs for Alaska public infrastructure at risk from climate. *Global Environmental Change*, pp. 442-457.

Lavin, P. (2003). *A Practical Guide to Design, Production, and Maintenance for Architects and Engineers.* London/New-York: Spon Press.

Law, Y., Ye, L., Pan, Y., & Yuan, Z. (2012). Nitrous oxide emissions from wastewater treatment processes. *Philosophical Transactions of the Royal Society B: Biological Sciences, 367(1593)*, pp. 1265-1277.

Linnerud, K., Mideksa, T. K., & Eskeland, G. S. (2011). The impact of climate change on nuclear power supply. *The Energy Journal, 32(1)*.

Lise, W., & van der Laan, J. (2015). Investment needs for climate change adaptation measures of electricity power plants in the EU. *Energy for Sustainable Development, 28*, pp. 10-20.

Mamo, G. E., Marence, M., Hurtado, J. C., & Franca, M. J. (2018). Optimization of Run-of-River Hydropower Plant Capacity.

Manoli, G., Fatichi, S., Schläpfer, M., Yu, K., Crowther, T. W., Meili, N., . . . Bou-Zeid, E. (2019). Magnitude of urban heat islands largely explained by climate and population. *Manoli, G., Fatichi, S., Schläpfer, M., Yu, K., Crowther, T. W., Meili, N., ... & Bou-Zeid, E. (2019). Magnitude of urban Nature, 573(7772)*, pp. 55-60.

Manwell, J. F., McGowan, J. G., & Rogers, A. L. (2010). *Wind energy explained: theory, design and application.* John Wiley & Sons.

Manwell, J., McGowan, J., & Rogers, A. (2002). *Wind Energy Explained: Theory, Design and Application.*

Maulbetsch, J. S., & Di Filippo, M. N. (2006). *Cost and value of water use at combined-cycle power plants.* California: California Energy Commission - Public Interest Energy Research Program.

Maupoux, M. (2010). *Solar photovoltaic water pumping.* Récupéré sur Practical Action - The Schumacher Centre for Technology and Development : https://sswm.info/sites/default/files/reference_attachments/MAUPOUX%202010%20Solar%20Water%20Pumping.pdf

Meral, M. E., & Dincer, F. (2011). A review of the factors affecting operation and efficiency of photovoltaic based electricity generation systems. *Renewable and Sustainable Energy Reviews, 15(5)*, pp. 2176-2184.

Mimikou, M. A., & Baltas, E. A. (1997). Climate change impacts on the reliability of hydroelectric energy production. *Hydrological Sciences Journal, 42(5)*, pp. 661-678.

Miradi, M. (2004). Artificial neural network (ANN) models for prediction and analysis of ravelling severity and material composition properties. *CIMCA*, pp. 892-903.

Mirgol, B., Nazari, M., & Eteghadipour, M. (2020). Modelling Climate Change Impact on Irrigation Water Requirement and Yield of Winter Wheat (Triticum aestivum L.), Barley (Hordeum vulgare L.), and Fodder Maize (Zea mays L.) in the Semi-Arid Qazvin Plateau, Iran. *Agriculture, 10(3), 60*.

Mourshed, M. (2012). Relationship between annual mean temperature and degree-days. *Energy and buildings, 54*, pp. 418-425.

N.D. Lea International. (1995). *Modelling Road Deterioration and Maintenance.* Prepared for the Asian Development Bank.

N.D. Lea International. (1995). *Modelling Road Deterioration and Maintenance.* Prepared for the Asian Development Bank.

National Snow & Ice Data Center. (n.d.). *freezing degree-days*. Retrieved from https://nsidc.org/cryosphere/glossary/term/freezing-degree-days

Nazahiyah, R., Yusop, Z., & Abustan, I. (2007). Stormwater quality and pollution loading from an urban residential catchment in Johor, Malaysia. *Water science and technology, 56(7)*, pp. 1-9.

Nemry, F., & Demirel, H. (2012). *Impacts of Climate Change on Transport: A focus on road and rail transport infrastructures.* Luxembourg: Publications Office of the European Union.

Nichol, J. E. (1996). High-resolution surface temperature patterns related to urban morphology in a tropical city: A satellite-based study. *Journal of applied meteorology, 35(1)*, pp. 135-146.

Nordhaus, W. (2017). Revisiting the social cost of carbon. *PNAS*, vol. 11, no.7, 1518-1523.

Nowak, D. J., Greenfield, E. J., Hoehn, R. E., & Lapoint, E. (2013). Carbon storage and sequestration by trees in urban and community areas of the United States. *Environmental pollution, 178, 229-236.*, pp. 229-236.

Ould-Amrouche, S., Rekioua, D., & Hamidat, A. (2010). Modelling photovoltaic water pumping systems and evaluation of their CO2 emissions mitigation potential. *Applied Energy, 87*, pp. 3451-3459.

Panagea, I. S., Tsanis, I. K., Koutroulis, A. G., & Grillakis, M. G. (2014). Climate change impact on photovoltaic energy output: the case of Greece. *Advances in Meteorology*.

Pande, P., & Telang, S. (2014). Calculation of Rainwater Harvesting Potential by Using Mean Annual Rainfall, Surface Runoff and Catchment Area. *Green Clean Guide, India, Global Advanced Research Journal of Agricultural Science, Vol 3(7)*, 200-204.

Parker, J. H. (1989, February). The impact of vegetation on air conditioning consumption. *In Proceedings of the Workshop on Saving Energy and Reducing Atmospheric Pollution by Controlling Summer Heat Islands (pp. 45-52).*

Parliamentary Office of Science and Technology (POST). (2011). *Carbon footprint of electricity generation.* Récupéré sur POST Note Update, 383:

https://www.parliament.uk/documents/post/postpn_383-carbon-footprint-electricity-generation.pdf

Pérez, G., Coma, J., Martorell, I., & Cabeza, L. F. (2014). Vertical Greenery Systems (VGS) for energy saving in buildings: A review. *Renewable and Sustainable Energy Reviews, 39*, pp. 139-165.

Petchers, N. (2003). *Combined heating, cooling & power handbook: technologies & applications: an integrated approach to energy resource optimization.* Fairmont Press.

Photovoltaic Softwares. (2020). *Photovoltaic Softwares*. Récupéré sur photovoltaic-software.com: https://photovoltaic-software.com/principle-ressources/how-calculate-solar-energy-power-pv-systems

Pierson Jr, W., & Moskowitz, L. (1964). A proposed spectral form for fully developed wind seas based on the similarity theory of SA Kitaigorodskii. *Journal of geophysical research*, pp. 5181-5190.

Plósz, B. G., Liltved, H., & Ratnaweera, H. (2009). Climate change impacts on activated sludge wastewater treatment: a case study from Norway. *Water Science and Technology, 60(2)*, pp. 533-541.

Poullain, J. (2012). *PDHonline Course H119 (2 PDH) - Estimating Storm Water Runoff.* Récupéré sur pdhonline.org: https://pdhonline.com/courses/h119/stormwater%20runoff.pdf

Prado, R. T., & Ferreira, F. L. (2005). Measurement of albedo and analysis of its influence the surface temperature of building roof materials. *Energy and Buildings, 37(4)*, 295-300.

Rademaekers, K., van der Laan, J., Boeve, S., Lise, W., van Hienen, J., Metz, B., . . . Kirchsteiger, C. (2011). *Investment needs for future adaptation measures in EU nuclear power plants and other electricity generation technologies due to effects of climate change .* Brussels: Library (DM28, 0/36).

Ramos-Scharron, C., & MacDonald, L. (2007). Runoff and suspended sediment yields from an unpaved road segment. *Hydrological Processes, 21(1)*, pp. 35-50.

Rodell, M., Chen, J., Kato, H., Famiglietti, J. S., Nigro, J., & Wilson, C. R. (2007). Estimating groundwater storage changes in the Mississippi River basin (USA) using GRACE. *Hydrogeology Journal 15[1]*, pp. 159-166.

Roorda, J., & van der Graaf, J. (2000). Understanding membrane fouling in ultrafiltration of WWTP-effluent. *Water Science and Technology 41(10-11)*, pp. 345-353.

Rousseau, Y. (2013). Impact of Climate Change on Thermal Power Plants. Case study of thermal power plants in France.

Sahely, H. R., MacLean, H. L., Monteith, H. D., & Bagley, D. M. (2006). Comparison of on-site and upstream greenhouse gas emissions from Canadian municipal wastewater treatment facilities. *Journal of Environmental Engineering and Science, 5(5)*, pp. 405-415.

Saito, I., Ishihara, O., & Katayama, T. (1990). Study of the effect of green areas on the thermal environment in an urban area. *Energy and buildings, 15(3-4)*, pp. 493-498.

Santamouris, M. (2014). Cooling the cities–a review of reflective and green roof mitigation technologies to fight heat island and improve comfort in urban environments. *Solar energy, 103*, pp. 682-703.

Scheehle, E. A., & Doorn, M. R. (2012). *Estimate of United States GHG Emissions from wastewater.* Récupéré sur EPA.org: https://www3.epa.gov/ttn/chief/conference/ei12/green/present/scheele.pdf

Scheehle, E. A., & Doorn, M. R. (2012). *Improvements to the U.S. Wastewater Methane and Nitrous Oxide Emissions.* Récupéré sur EPA.org: https://www3.epa.gov/ttn/chief/conference/ei12/green/scheehle.pdf

Schnetzer, J., & Pluschke, L. (2017). *Solar-Powered Irrigation Systems: A clean-energy, low-emission option for irrigation development and modernization.* FAO.

Shukla, A. K., & Singh, O. (2014). Effect of Compressor Inlet Temperature & Relative Humidity on Gas Turbine Cycle Performance. *International Journal of Scientific & Engineering Research, 5(5)*, 664-670.

Shukla, A. K., & Singh, O. (2014). Effect of Compressor Inlet Temperature & Relative Humidity on Gas Turbine Cycle Performance. *International Journal of Scientific & Engineering Research, 5(5)*, 664-670.

Singh, S., & Kumar, R. (2012). Ambient air temperature effect on power plant performance. *International Journal of Engineering Science and Technology*.

Singh, S., & Tiwari, S. (2019). *Climate Change, Water and Wastewater Treatment: Interrelationship and Consequences.* Singapore: Springer.

Song, Z., Zheng, Z., Li, J., Sun, X., Han, X., Wang, W., & Xu, M. (2006). Seasonal and annual performance of a full-scale constructed wetland system for sewage treatment in China. *Ecological Engineering, 26(3)*, pp. 272-282.

Souch, C. A., & Souch, C. (1993). The effect of trees on summertime below canopy urban climates: a case study Bloomington. *Journal of Arboriculture, 19(5)*, pp. 303-312.

Taha, H. (1996). Modeling impacts of increased urban vegetation on ozone air quality in the South Coast Air Basin. *Atmospheric Environment, 30(20)*, pp. 3423-3430.

Taha, H. (1997). Urban climates and heat islands; albedo, evapotranspiration, and anthropogenic heat. *Energy and buildings, 25(2).*

Taha, H., Akbari, H., & Rosenfeld, A. (1988). Vegetation Canopy Micro-Climate: A Field-Project in Davis, California. *Journal of Climate and Applied Meteorology*.

Taha, H., Akbari, H., & Rosenfeld, A. (1991). Heat island and oasis effects of vegetative canopies: micro-meteorological field-measurements. *Theoretical and Applied Climatology, 44(2)*, pp. 123-138.

Tallis, M., Taylor, G., Sinnett, D., & Freer-Smith, P. (2011). Estimating the removal of atmospheric particulate pollution by the urban tree canopy of London, under current and future environments. *Landscape and Urban Planning, 103(2)*, pp. 129-138.

Tang, H. (2012). Research on Temperature and Salt Migration Law of Sulphate Salty Soil Subgrade in Xinjiang Region. Beijing, China: Beijing Jiaotong University.

Taylor, C. R., Hook, P. B., Stein, O. R., & Zabinski, C. A. (2011). Seasonal effects of 19 plant species on COD removal in subsurface treatment wetland microcosms. *Ecological Engineering, 37(5)*, pp. 703-710.

Tiwary, A., Sinnett, D., Peachey, C., Chalabi, Z., Vardoulakis, S., Fletcher, T., . . . Hutchings, T. R. (2009). An integrated tool to assess the role of new planting in PM10 capture and the human health benefits: A case study in London. *Environmental pollution, 157(10)*, pp. 2645-2653.

Tran, Q. K., Jassby, D., & Schwabe, K. A. (2017). The implications of drought and water conservation on the reuse of municipal wastewater: Recognizing impacts and identifying mitigation possibilities. *Water research, 124*, 472-481.

Tsihrintzis, V. A., & Hamid, R. (1998). Runoff quality prediction from small urban catchments using SWMM. *Hydrological Processes, 12(2)*, pp. 311-329.

U.S. DoE. (2013). *U.S. Energy sector vulnerabilities to climate change and extreme weather.* DOE/PI-0013: U.S. Department of Energy.

U.S. Environmental Protection Agency. (2003, September). *Cooling summertime temperatures: Strategies to reduce heat islands.* Récupéré sur epa.gov: https://www.epa.gov/sites/production/files/2014-06/documents/hiribrochure.pdf

Ullrich, A., & Volk, M. (2009). Application of the Soil and Water Assessment Tool (SWAT) to predict the impact of alternative management practices on water quality and quantity. *Agricultural Water Management, 96(8)*, pp. 1207-1217.

UNEP. (2015). *Economic Valuation of Wastewater - The Cost of Action and the Cost of No Action.* United Nations Environment Programme (UNEP), commissioned by the Global Programme of Action for the Protection of the Marine Environment from Land-based Activities (GPA), through the Global Wastewater Initiative (GW2I).

URS Corporation Limited. (2010). *Adapting Energy, Transport and Water Infrastructure to the Long-term Impacts of Climate Change .* San Francisco, CA, USA, Report RMP/5456.

Valkama, P., Mäkinen, E., Ojala, A., Vahtera, H., Lahti, K., Rantakokko, K., . . . Wahlroos, O. (2017). Seasonal variation in nutrient removal efficiency of a boreal wetland detected by high-frequency on-line monitoring. *Ecological engineering, 98*, pp. 307-317.

Van Vliet, M. T., Yearsley, J. R., Ludwig, F., Vögele, S., Lettenmaier, D. P., & Kabat, P. (2012). Vulnerability of US and European electricity supply to climate change. *Nature Climate Change, 2(9)*, 676-681.

Vought, T. D. (2019, June 30). *An Economic Case for Facility Lightning Protection Systems in 2017*. Récupéré sur VFC: https://vfclp.com/articles/an-economic-case-for-facility-lightning-protection-systems-in-2017/

Watkins, R., Littlefair, P., Kolokotroni, M., & Palmer, J. (2002). The London heat island–Surface and air temperature measurements in a park and street gorges. *ASHRAE Transactions, 108(1)*, pp. 419-427.

Wilbanks, T., Bhatt, V., Bilello, D., Bull, S., Ekmann, J., Horak, W., & Huang, Y. J. (2008). *Effects of Climate Change on Energy Production and Use in the United States.* Lincoln: US Department of Energy Publications.

Xiao, Q., & McPherson, E. G. (2002). Rainfall interception by Santa Monica's municipal urban forest. *Urban ecosystems, 6(4)*, pp. 291-302.

Yamba, F., Walimwipi, H., Jain, S., Zhou, P., Cuamba, B., & Mzezewa, C. (2011). Climate change/variability implications on hydroelectricity generation in the Zambezi River Basin. *Mitigation and Adaptation Strategies for Global Change*, pp. 617-628.

Young, I. R., & Holland, G. J. (1996). Atlas of the oceans: wind and wave climate. *Oceanographic Literature Review, 7(43), 742*.

Yuan, H., Nie, J., Zhu, N., Miao, C., & Lu, N. (2013). Effect of temperature on the wastewater treatment of a novel anti-clogging soil infiltration system. *Ecological engineering, 57*, pp. 375-379.

Zhang, C., Liao, H., & Mi, Z. (2019). Climate impacts: temperature and electricity consumption. *Natural Hazards, 99(3)*, pp. 1259-1275.

Zhang, Y., Kendy, E., Qiang, Y., Changming, L., Yanjun, S., & Hongyong, S. (2004). Effect of soil water deficit on evapotranspiration, crop yield, and water use efficiency in the North China Plain. *Agricultural Water Management, 64*(2), pp. 107-122.

Zhao, C., Liu, B., Piao, S., Wang, X., Lobell, D., Huang, Y., ... (2017). Temperature increase reduces global yields of major crops in four independent estimates. *Proceedings of the National Academy of Sciences, 114 (35)*. doi:https://doi.org/10.1073/pnas.1701762114

Zhao, M., Kong, Z. H., Escobedo, F. J., & Gao, J. (2010). Impacts of urban forests on offsetting carbon emissions from industrial energy use in Hangzhou, China. *Journal of Environmental Management, 91(4)*, pp. 807-813.

Zhao, X., Shen, A., & Ma, B. (2018). Temperature Adaptability of Asphalt Pavement to High Temperatures and Significant Temperature Differences. *Advances in Materials Science and Engineering*.

Zheng, S., Huang, G., Zhou, X., & Zhu, X. (2020). Climate-change impacts on electricity demands at a metropolitan scale: A case study of Guangzhou, China. *Applied Energy, 261, 114295*.

Zhou, Z. C., Shangguan, Z. P., & Zhao, D. (2006). Modeling vegetation coverage and soil erosion in the Loess Plateau Area of China. *Ecological modelling, 198(1-2)*, pp. 263-268.

Zoppou, C. (2001). Review of urban storm water models. *Environmental Modelling & Software, 16(3)*, pp. 195-231.

Zouboulis, A., & Tolkou, A. (2016). Effect of climate change in wastewater treatment plants: reviewing the problems and solutions. Dans S. A. Shrestha, *Managing Water Resources under Climate Uncertainty* (pp. 197-220). Springer.

Zoulia, I., Santamouris, M., & Dimoudi, A. (2009). Monitoring the effect of urban green areas on the heat island in Athens. *Environmental monitoring and assessment, 156(1-4)*.

Zsirai, T., Buzatu, P., Maffettone, R., & Judd, S. (2012, April). *Sludge viscosity—The thick of it*. Récupéré sur The MBR (Membrane Bioreactors): https://www.thembrsite.com/features/sludge-viscosity-in-membrane-bioreactors-the-thick-of-it/

Annex I: Code for establishing the CDS Toolbox-SAVi link

Code related to offline processing of CDS Toolbox and CDS API data for the C3S_428h_IISD-EU project.

How does this code relate to the CDS API ?

This code builds on the powerful CDS API but focuses on local impact analysis specific for the C3S_428h_IISD-EU project. It makes it easier to retrieve a time series for a specific location or region, and save the result to a CSV file (a simpler format than netCDF for most climate adaptation practitioners). Additionally, the code combines variables across multiple datasets, aggregate them into asset classes (such as all energy-related variables) and perform actions such as bias correction (use of ERA5 and CMIP5).

Code available for download

The easy way is to download the zipped archive: - latest (development): https://github.com/perrette/iisd-cdstoolbox/archive/master.zip - or check stable releases with description of changes: https://github.com/perrette/iisd-cdstoolbox/releases (see assets at the bottom of each release to download a zip version)

The hacky way is to use git (only useful during development, for frequent updates, to avoid having to download and extract the archive every time):

- First time: `git clone https://github.com/perrette/iisd-cdstoolbox.git`

- Subsequent updates: `git pull` from inside the repository

Installation steps

- Download the code (see above) and inside the folder.
- Install Python 3, ideally Anaconda Python which comes with pre-installed packages
- Install the CDS API key: https://cds.climate.copernicus.eu/api-how-to
- Install the CDS API client: pip install cdsapi
- Install other dependencies: conda install --file requirements.txt or pip install -r requirements.txt
- *Optional* dependency for coastlines on plots: conda install -c conda-forge cartopy or see docs
- *Optional* dependency: CDO (might be needed later, experimental): conda install -c conda-forge python-cdo

Troubleshooting: - If install fails, you may need to go through the dependencies in requirements.txt one by one and try either pip install or conda install or other methods specific to that dependency. - In the examples that follow, if you have both python2 and python3 installed, you might need to replace python with python3.

CDS API

Download indicators associated with one asset class.

Examples of use:

```
python download.py --asset energy --location Welkenraedt
```

The corresponding csv time series will be stored in `indicators/welkenraedt/energy`. Note that raw downloaded data from the CDS API (regional tiles in netcdf format, and csv for the required lon/lat, without any correction) are stored under `download/` and can be re-used across multiple indicators.

The `indicators` folder is organized by location, asset class, simulation set and indicator name. The aim is to provide multiple sets for SAVi simulation. For instance, `era5` for past simulations, and various `cmip5` versions for future simulations, that may vary with model and experiment. For instance the above command creates the folder structure (here a subset of all variables is shown):

```
indicators/
  welkenraedt/
    energy/
      era5/
        2m_temperature.csv
        precipitation.csv
        ...
      cmip5-ipsl_cm5a_mr-rcp_8_5/
        2m_temperature.csv
        precipitation.csv
        ...
      ...
```

with two simulation sets `era5` and `cmip5-ipsl_cm5a_mr-rcp_8_5`. It is possible to specify other models and experiment via `--model` and `--experiment` parameters, to add further simulation sets and thus test how the choice of climate models and experiment affect the result of SAVi simulations.

Compared to raw CDS API, some variables are renamed and scaled so that units match and are the same across simulation sets. For instance, temperature was adjusted from Kelvin to degree Celsius, and precipitation was renamed and units-adjusted into mm per month from original (mean_total_precipitation_rate (mm/s) in ERA5, and mean_precipitation_flux (mm/s) in CMIP5). Additionally, CMIP5 data is corrected so that climatological mean matches with ERA5 data (climatology computed over 1979-2019 by default).

Additionally to the files shown in the example folder listing above, figures can also be created for rapid control of the data, either for interactive viewing (`--view-timeseries` and `--view-region`) or or saved as PNG files (`--png-timeseries` and `--png-region`), e.g.

```
python download.py --asset energy --location Welkenraedt --png-timeseries --
png-region
```

Single indicators can be downloaded via:

```
python download.py --indicator 2m_temperature --location Welkenraedt
```

The choices available for `--indicator` , `--asset` and `--location` area defined in the following configuration files, respectively:

- controls which indicators are available, how they are renamed and unit-adjusted: indicators.yml (see sub-section below)
- controls the indicator list in each asset class: assets.yml
- controls the list of locations available: locations.yml

Full documentation, including fine-grained controls, is provided in the command-line help:

```
python download.py --help
```

Visit the CDS Datasets download pages, for more information about available variables, models and scenarios:

- ERA5: https://cds.climate.copernicus.eu/cdsapp#!/dataset/reanalysis-era5-single-levels-monthly-means?tab=form

- CMIP5: https://cds.climate.copernicus.eu/cdsapp#!/dataset/projections-cmip5-monthly-single-levels?tab=form

In particular, clicking on “Show API request” provides information about spelling of the parameters, e.g. that “2m temperature” is spelled `2m_temperature` and “RCP 8.5” is spelled `rcp_8_5`.

Indicator definition

This section is intended for users who wish to extend the list of indicators currently defined in indicators.yml. It can be safely ignored for users who are only interested in using the existing indicators.

Let’s see how `10m_wind_speed` is defined:

```
- name: 10m_wind_speed
  units: m / s
  description: Wind speed magnitude at 10 m
```

The fields `name` and `units` define the indicator. Description is optional, just to provide some context. It is possible to provide `scale` and `offset` fields to correct the data as `(data + offset) * scale`. Here for `2m temperature`:

```
- name: 2m_temperature
  units: degrees Celsius
  description: 2-m air temperature
  offset: -273.15  # Kelvin to degrees C
```

# denotes a comment to provide some context. Some indicators have different names in ERA5 and CMIP5, and possibly different units. That can be dealt with by providing `era5` and `cmip5` fields, which have precedence over the top-level fields. Here the `evaporation` definition:

```
- name: evaporation
  units: mm per month
  era5:
    name: mean_evaporation_rate  # different name in ERA5
    scale: -2592000  # change sign and convert from mm/s to mm / month
  cmip5:
    scale: 2592000  # mm/s to mm / month
```

In that case both scaling and name depend on the dataset. In CMIP5 which variable name is identical to our indicator name, the `name` field can be omitted. In ERA5, evaporation is negative (downwards fluxes are counted positively), whereas it is counted positively in ERA5.

Indicators composed of several CDS variables can be defined via `compose` and `expression` fields. Let's look at `100m_wind_speed`:

```
- name: 100m_wind_speed
  units: m / s
  description: Wind speed magnitude at 100 m
  era5:
    compose:
      - 100m_u_component_of_wind
      - 100m_v_component_of_wind
    expression: (_100m_u_component_of_wind**2 + _100m_v_component_of_wind**2)
**0.5
  cmip5:
    name: 10m_wind_speed
    scale: 1.6  # average scaling from 10m to 100m, based on one test locatio
n (approximate!)
```

In ERA5, vector components of 100m wind speed are provided. Our indicator is therefore a composition of these two variables, defined by the `expression` field, which is evaluated as a python expression. Note that variables that start with a digit are not licit in python and must be prefixed with an underscore _ in the `expression` field (only there).

For complex expressions, it is possible to provide a `mapping` field to store intermediate variables, for readability. This is used for the `relative_humidity` indicator:

```
- name: relative_humidity
  units: '%'
  era5:
    compose:
```

```
      - 2m_temperature
      - 2m_dewpoint_temperature
    expression: 100*(exp((17.625*TD)/(243.04+TD))/exp((17.625*T)/(243.04+T)))
    mapping: {T: _2m_temperature - 273.15, TD: _2m_dewpoint_temperature - 273
.15}
  cmip5:
    name: near_surface_relative_humidity
```

where `T` and `TD` are provided as intermediary variables, to be used in `expression`.

ERA5-hourly dataset can be retrieved via `frequency: hourly` field, and subsequently aggregated to monthly indicators thanks to pre-defined functions `daily_max`, `daily_min`, `daily_mean`, `monthly_mean`, `yearly_mean`. For instance:

```
- name: maximum_daily_temperature
  units: degrees Celsius
  offset: -273.15
  cmip5:
    name: maximum_2m_temperature_in_the_last_24_hours
  era5:
    name: 2m_temperature
    frequency: hourly
    transform:
      - daily_max
      - monthly_mean
```

This variable is available directly for CMIP5, but not in ERA5. It is calculated from `2m_temperature` from ERA5 `hourly` dataset, and subsequently aggregated. Note the ERA5-hourly dataset takes significantly longer to retrieve than ERA5 monthly. Consider using in combination with `--year 2000` to retrieve a single year of the ERA5 dataset.

Currently CMIP5 daily is not supported.

Netcdf to csv conversion

Convert netcdf time series files downloaded from the CDS Toolbox pages into csv files (note: this does not work for netcdf files downloaded via the cds api):

```
python netcdf_to_csv.py data/*nc
```

Help:
```
python netcdf_to_csv.py --help
```

Copernicus Climate Change Service